JOURNAL OF PETROLOGY

*Journal of Petrology*, 2016, Vol. 56, No. 12, 2319–2340
doi: 10.1093/petrology/egv075
Advance Access Publication Date: 27 January 2016
Original Article

OXFORD

# Magma Chamber Processes in the Formation of the Low-sulphide Magmatic Au–PGE Mineralization of the Platinova Reef in the Skaergaard Intrusion, East Greenland

**Reid R. Keays[1,*] and Christian Tegner[2]**

[1]School of Earth, Atmosphere and Environment, Monash University, Clayton, VIC 3800, Australia and [2]Geoscience, University of Aarhus, DK-8000, Aarhus, Denmark

*Corresponding author. E-mail: Reid.Keays@monash.edu

Received September 29, 2014; Accepted November 27, 2014

## ABSTRACT

The Platinova Reef comprises a series of platinum group element (PGE)- and Au-rich layers that contain precious metals intimately associated with magmatic Cu-rich sulphides. This study presents new PGE, Au, S, Se and Te data for samples collected along a stratigraphic reference section from the base of the Lower Zone up to the Sandwich Horizon of the Skaergaard intrusion, and seeks to address the magma chamber processes that led to the formation of the Platinova Reef. The majority of the Skaergaard rocks have low S contents (<500 ppm), with the S contents of those within and below the Platinova Reef being especially low (<100 ppm). The very low S contents of these rocks are due in large part to the low S content of the initial Skaergaard magma; there is no evidence for any post-magmatic S loss in this part of the stratigraphy. Rayleigh fractionation modelling of the variations in metal concentrations of samples from this stratigraphic reference section indicates that the initial Skaergaard magma contained 240 ppm Cu, 89 ppm S, 4·0 ppb Au, 18·7 ppb Pd, 9 ppb Pt, 90 ppb Se and 5·7 ppb Te. The high Pd/Pt ratio of the Skaergaard magma indicates that it had undergone a considerable amount of differentiation prior to its entry into the Skaergaard magma chamber. Precious metal enrichment commenced at a stratigraphic level ~300 m below the Platinova Reef owing to saturation of the magma in Au–PGE-rich Cu sulphides. Although only tiny amounts of sulphides were initially formed, precious metal enrichment increased rapidly upwards to culminate in the formation of the Platinova Reef. Sulphide saturation of the magma was initially restricted to the boundary layer between the magma and the crystal mush where cumulus Fe–Ti oxides were forming. Although only very small amounts of sulphides were initially formed, the rate of sulphide production increased with time, leading to the entire residual magma in the chamber becoming sulphide saturated immediately after the formation of the Platinova Reef. Sulphide saturation and the eventual formation of the Au–PGE mineralization in the Reef was the product of a number of important factors. These include prolonged fractionation of the magma, which produced a residual melt that was enriched in Au, Pd, Cu, S and FeO and led to the build-up and eventual saturation of the magma in Fe–Ti oxides and Cu sulphides. The formation of cumulus ilmenite and magnetite slowed down the rate of build-up of FeO in the magma and also removed $O_2$ and caused some of the $SO_4^{2-}$ in the residual magma to be converted to $S^{2-}$, whereas the high Cu content (621 ppm calculated from Rayleigh fractionation modelling) of the residual magma at this stage drove the magma to sulphide saturation, forming very small amounts of immiscible PGE–Au-rich Cu sulphides. Other factors that contributed to sulphide saturation of the magma

were decreases in temperature and $fO_2$ of the magma, which were accompanied by an increase in the $SiO_2$ concentrations of the residual melt.

**Key words**: Skaergaard; Platinova Reef; magmatic Au–PGE; sulphide saturation; ore genesis

## INTRODUCTION

The Skaergaard intrusion, which is one of the world's most studied gabbroic intrusions (Nielsen, 2004; Tegner *et al.*, 2009), hosts significant amounts of Au–PGE mineralization in what is known as the Platinova Reef. Although most researchers (e.g. Bird *et al.*, 1991; Andersen *et al.*, 1998; Andersen, 2006) agree that the mineralization is primary in origin and that the Au–PGE mineralization is intimately associated with magmatic sulphides, the Skaergaard rocks within and below the Platinova Reef contain very low quantities of sulphides (Wager *et al.*, 1957; Turner, 1986; Andersen, 2006; Keays *et al.*, 2008). A fundamental question is whether the parental Skaergaard magma had a low S content or whether S was lost at some post-magmatic stage. Evidence that the parental Skaergaard magma had a low S content is provided by the low S contents of samples from its chilled margins. Additionally, the Skaergaard complex is almost certainly co-magmatic with the high-$TiO_2$ continental flood basalts of East Greenland (Jakobsen *et al.*, 2010; Wotzlaw *et al.*, 2012), which Momme *et al.* (2002) concluded had been formed from low-S magmas. However, Andersen (2006) concluded on the basis of modelling that the parental Skaergaard magma contained 894 ppm S but that there had been massive S losses from the lower portions of the Skaergaard intrusion, within and below the Platinova Reef, at some post-magmatic stage. If the primary Skaergaard magma was sulphide undersaturated, what process or processes drove the magma to sulphide saturation and the formation of PGE-rich magmatic sulphides?

In this study, we present geochemical data for samples from a stratigraphic reference section from the exposed base of the Skaergaard intrusion up to the Sandwich Horizon (Tegner *et al.*, 2009). We examine the processes that drove the Skaergaard magma to sulphide saturation and associated mineralization, and show that major changes in the geochemistry of the platinum group elements (PGE) and their decoupling from the lithophile trace elements began ~300 m stratigraphically below the Platinova Reef. We also address the issue of whether or not there was post-magmatic S loss as suggested by Andersen (2006).

### Geological setting

The Skaergaard intrusion formed as part of the North Atlantic Large Igneous Province. Although magmatism within the East Greenland rifted margin spanned tens of millions of years from 61 to 14 Ma, the vast majority of the magmas erupted as an enormous flood basalt succession at ~55 Ma coinciding with continental rupture between Greenland and Eurasia (Pedersen *et al.*, 1997; Storey *et al.*, 2004, 2007). The Skaergaard intrusion was emplaced partly into the base of these flood basalts and partly into the underlying Precambrian gneissic basement (Fig. 1). Chronology (Hirschmann *et al.*, 1997; Wotzlaw *et al.*, 2012) and geochemistry (Brooks & Nielsen, 1978; Nielsen, 2004; Jakobsen *et al.*, 2010) link Skaergaard to the flood basalt event. Moreover, fluid inclusions demonstrate that the Skaergaard magma chamber subsided while crystallizing as a consequence of rapid emplacement of the flood basalts over the magma chamber (Larsen & Tegner, 2006). The corollary of these constraints, combined with those on the cooling history of Skaergaard (Taylor & Forester, 1979), is that the main flood basalt event took less than 300 kyr (Larsen & Tegner, 2006). Such anomalous volcanic productivity is best explained by melting of hot mantle plume material and has been associated with the initiation of the Iceland hotspot (Wilson, 1973; White & McKenzie, 1989; Storey *et al.*, 2007). This is corroborated not only by the enrichment of the Skaergaard magma and the flood basalts in Fe, Ti and incompatible trace elements relative to mid-ocean ridge basalts (MORB) (Tegner *et al.*, 1998; Nielsen, 2004; Jakobsen *et al.*, 2010) but also by the similarity of the isotopic compositions of basalts in East Greenland and Iceland (McBirney & Creaser, 2003; Peate & Stecher, 2003; Peate *et al.*, 2003; Barker *et al.*, 2006). Moreover, Momme *et al.* (2002) showed that the ferrobasalts associated with Skaergaard were distinctly sulphur undersaturated and enriched in PGE (e.g. 6–16 ppb Pd) and subsequently ascribed this to melting of hot plume mantle below a thick lithospheric lid (Momme *et al.*, 2006).

The Skaergaard intrusion is divided into three main series (Fig. 2), the Layered Series, the Upper Border Series and the Marginal Border Series, which crystallized respectively on the floor, roof and walls of the chamber (Wager & Brown, 1968; Naslund, 1984; Hoover, 1989; McBirney, 1995). The three series are divided into Lower Zone (LZ), Middle Zone (MZ) and Upper Zone (UZ) equivalents based on the presence, disappearance and subsequent reappearance of primocryst olivine, respectively, and are further subdivided into subzones based on the appearance of new mineral phases as outlined in Fig. 2. The plagioclase core compositions at subzone boundaries show similar An% in the three series, suggesting that the intrusion solidified from the margins inwards by *in situ* crystallization in a crystal mush boundary layer along the floor, walls and roof of a homogeneous magma body (Hoover, 1989;

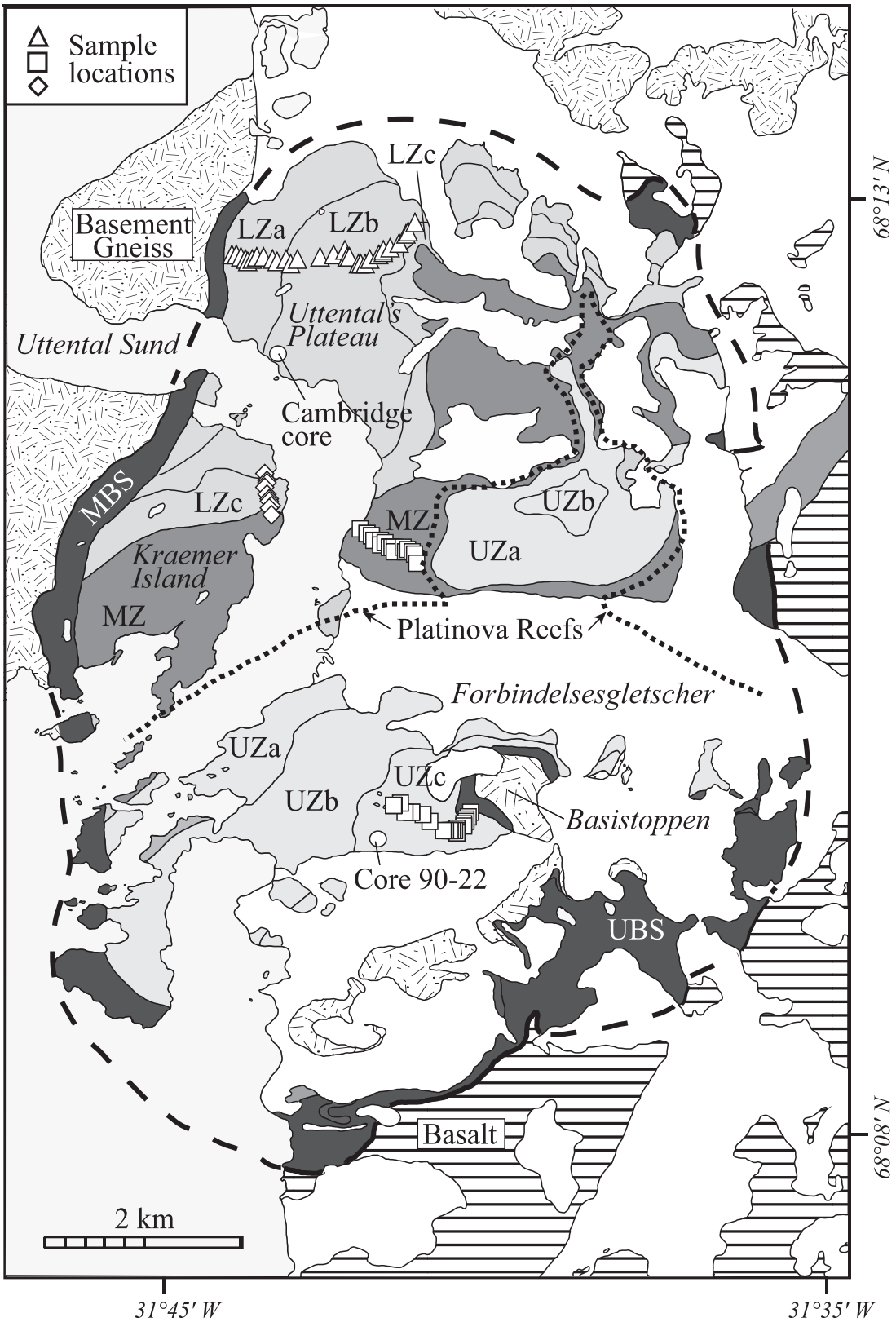


**Fig. 1.** Geological map of the Skaergaard intrusion showing the locations of surface samples and the position of diamond drill hole core 90-22. LZ, Lower Zone; MZ, Middle Zone; UZ, Upper Zone; MBS, Marginal Border Series; UBS, Upper Border Series. Modified after Tegner *et al.* (2009).

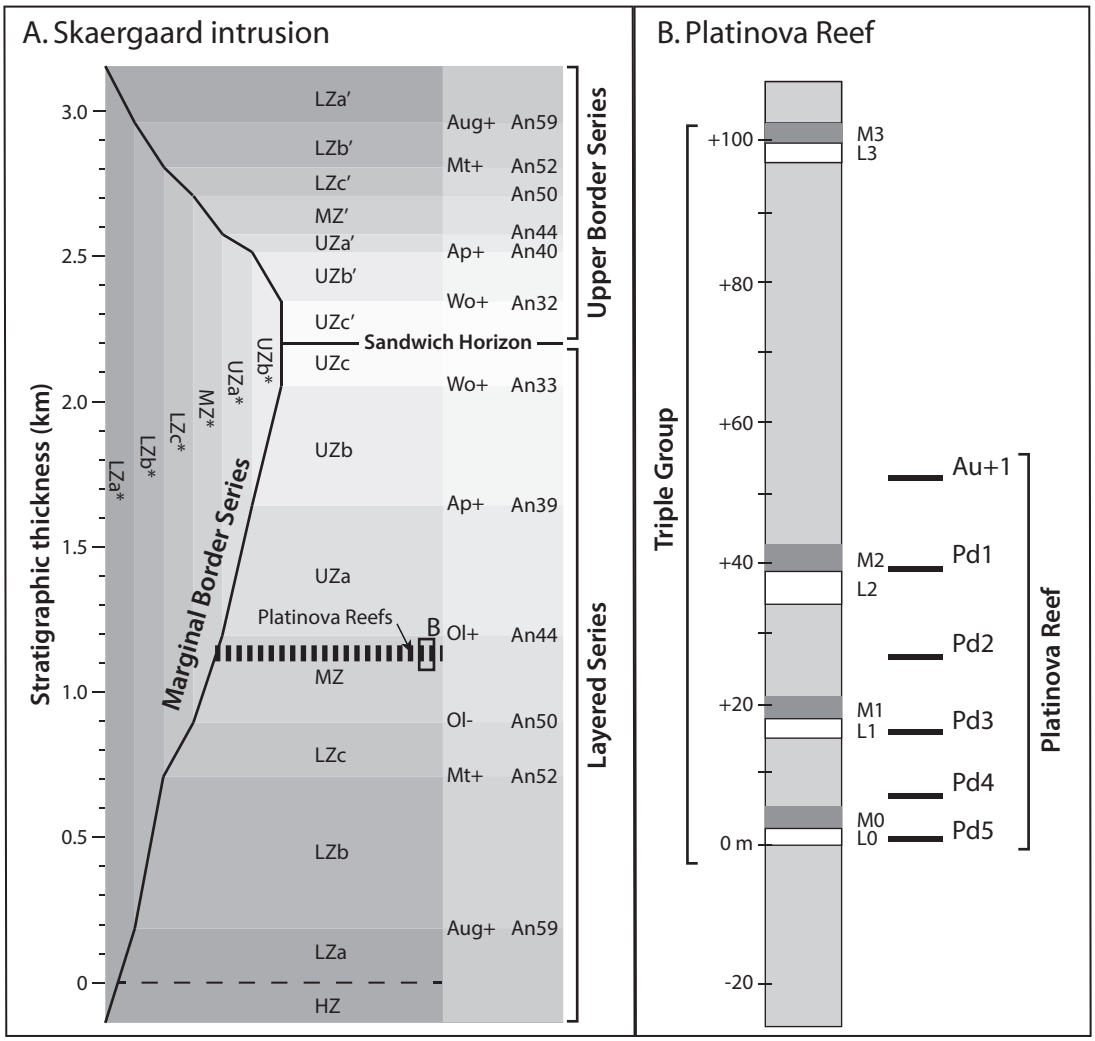


**Fig. 2.** (a) Stratigraphic column for the Skaergaard intrusion showing the position of the Platinova Reef; modified after Salmonsen & Tegner (2013). (b) Detailed stratigraphy of the Platinova Reef; modified after Holwell & Keays (2014). The Triple Group as defined by Wager & Deer (1939) incorporates leucocratic layers L1, L2 and L3. Bird *et al.* (1991) extended the definition of the Triple Group to include leucocratic layer L0 as well as melanocratic layers M0, M1, M2 and M3. Abbreviations as in Fig. 1.

Salmonsen & Tegner, 2013). The most important subzone boundaries for this study are between LZb and LZc where ilmenite and magnetite start to crystallize as cumulus phases and between LZc and MZ where olivine ceases to be a cumulus phase (Wager & Brown, 1968); these levels are located *c.* 310 m and *c.* 160 m, respectively, below the Platinova Reef (Fig. 2).

The Platinova Reef is up to 60 m thick, occurs in the upper part of the MZ of the Layered Series (Fig. 2), and consists of a series of distinct Au–PGE-rich stratiform zones or layers that are PGE-rich at the base and become progressively Au-rich towards the top (Bird *et al.*, 1991; Andersen *et al.*, 1998; Nielsen *et al.*, 2005; Holwell & Keays, 2014). Compared with most other stratiform PGE mineralization within layered intrusions, the Platinova Reef is hosted in evolved oxide gabbros formed by prolonged fractional crystallization of parental basalt. Based on the mass proportions of Nielsen (2004), the Platinova Reef formed after 75% crystallization by mass of the parental magma, which itself had evolved by perhaps 50% crystallization from a primary mantle derived basaltic melt. The Platinova Reef occurs in what has been long known as the Triple Group; this consists of three prominent, continuous leucocratic layers, which together with melanocratic layers form stratigraphic packages (Wager & Deer, 1939; Andersen *et al.*, 1998). The leucocratic layers are designated L1, L2 and L3 from the base upwards. A striking feature of the PGE mineralization is that the strongest Pd enrichment occurs in a less prominent leucrocratic layer below L1, designated L0 by Holwell & Keays (2014) and TG-$O_L$ by Andersen *et al.* (1998); the major Pd layer occurs in exactly the same leucocratic layer (L0) across the intrusion.

Most of the gabbros of the LZ and MZ of the Layered Series contain few sulphides, about 0·02 wt % (Wager *et al.*, 1957). The dominant sulphides are bornite and digenite, plus minor chalcopyrite associated with magnetite and ilmenite (Wager *et al.*, 1957; Andersen *et al.*, 1998); if present in equal proportions, the bornite and

digenite would have contributed ~0·005 wt % S or 50 ppm S to the rocks. Whereas most magnetite in the intrusion is titaniferous, that associated with the sulphides has a low $TiO_2$ content (Andersen *et al.*, 1998). The gabbros in the Upper Zone contain about 2 wt % sulphides, mainly pyrrhotite plus minor chalcopyrite, but no bornite (Wager *et al.*, 1957). Wager *et al.* (1957) concluded that the Skaergaard magma began to segregate a Cu-rich sulphide melt when the Cu and S contents of the magma had increased to 0·02 and 0·01 wt %, respectively. Andersen *et al.* (1998) and Andersen (2006) suggested that the sulphides in the lower portions of the Skaergaard intrusion were originally pyrrhotite and chalcopyrite that were converted to bornite and digenite assemblages during later oxidation and desulphurization. Andersen (2006) further suggested that the sulphide content of the Lower Zone was 0·07 modal % (= 0·04 wt % S) and that S liberated during oxidation of the sulphides in the Lower Zone was deposited in the Upper Zone, where it formed pyrrhotite. Support for this suggestion is the extensive subsolidus oxidation and re-equilibration of the Fe–Ti oxide minerals at temperatures between 500 and 900°C (Buddington & Lindsley, 1964; Bollingberg, 1995).

## SAMPLING STRATEGY AND ANALYTICAL METHODS

The samples investigated in this study were collected along a stratigraphic reference section from the exposed base of the Skaergaard intrusion to a position just below the Sandwich Horizon in the upper part of the Layered Series, as well as from diamond drill hole core 90-22 (Fig. 1; Tegner *et al.*, 2009). A total of 52 samples were investigated, including 20 closely spaced samples across the Platinova Reef (drill core 90-22) for which Bernstein & Nielsen (2004) have previously reported Pd, Pt and Au data.

The 32 samples for which Ir, Ru, and Rh data are reported in Supplementary Data Table 1 (supplementary data are available for downloading at http://www.petrology.oxfordjournals.org), together with Pd, Pt and Au, were analysed at the low-level PGE facility of the Geoscience Laboratories in Sudbury, following procedures described by Jackson *et al.* (1990) and Keays & Lightfoot (2004). Fifteen grams of powdered rock were mixed with sodium carbonate, sulphur, silica flour and Ni powder. This mixture was baked at 1050°C for 1·5 h in a fire-clay crucible. After dissolution of the Ni–sulphide button, the PGE were collected by Te co-precipitation, re-dissolved in acid, and the concentrations were determined by inductively coupled plasma–mass spectrometry. The detection limits (in ppb) for these analyses are: Ir (0·04), Ru (0·13), Rh (0·08), Pt (0·14), Pd (0·11), and 0·71 (Au). The Pt, Pd, and Au data for the remaining 20 samples were determined at Activation Laboratories in Canada and previously reported by Bernstein & Nielsen (2004). The Se and Te contents of all samples were determined in the Sudbury Geoscience Laboratories using a hydride generator followed by atomic absorption spectroscopy; the detection limits for the method were 3·5 ppb Se and 1·0 ppb Te. The S contents of 32 samples were determined at the Geoscience Laboratories using an infra-red technique (Leco) with a detection limit of 100 ppm S. Five of these samples were also analysed by mass spectrometry at the University of Indiana using the method described by Ripley *et al.* (2011) with a detection limit of 15 ppm. The remaining major and trace element concentrations were analysed by X-ray fluorescence and reported by Tegner *et al.* (2009).

The Layered Series contains abundant autoliths of troctolite, gabbroic anorthosite, and oxide (magnetite–ilmenite) gabbro, broken and sunken from parts of the Upper Border Series of the intrusion (Irvine *et al.*, 1998). One such autolith, a leucogabbro collected along the stratigraphic reference section at 900 m, was analysed in this study.

Representative analyses are given in Table 1 and the entire dataset is given in Supplementary Data Table 1.

## RESULTS

In the analysed subset of samples, there is a slight decrease in $TiO_2$ content from the base of LZa to the base of LZc, at 703 m, followed by a sharp increase in $TiO_2$ up to 988 m, just above the base of MZ; this is followed by a sharp decrease to immediately below the Platinova Reef package at 1024 m (Fig. 3a). The sharp increase in $TiO_2$ above the base of LZc marks the first appearance of cumulus magnetite (Wager & Brown, 1968). Within the Reef package, $TiO_2$ values fluctuate between 3·5 and 10·5 wt %, reflecting modal magnetite variations; subsequently there is a steady decline in $TiO_2$ contents through the Upper Zone (Fig. 3a).

Total Fe contents, expressed as $FeO_T$, have a similar distribution to $TiO_2$ contents to the top of the Reef package (Fig. 3b); however, above the Reef $FeO_T$ contents continue to increase, reaching 30 wt % $FeO_T$ at the base of UZc. The rapid increase in $FeO_T$ above the base of LZc and the lower values above 900 m exactly mirror the case of $TiO_2$.

Because the S capacity of magmas is affected by both their FeO contents and their $fO_2$ (Haughton *et al.*, 1974), it is important to know much magnetite fractionated as well as the $FeO_T$ contents of the rocks. A good proxy for magnetite is V, which is strongly partitioned into magnetite but not into ilmenite; although V also partitions into clinopyroxene, $D_V$ magnetite/silicate melt (= 26) is considerably higher than $D_V$ clinopyroxene/silicate melt (= 1·35) (Rollinson, 1993). The distribution pattern of V in the Skaergaard rocks up to the top of the Middle Zone is similar to that of both $FeO_T$ and $TiO_2$ (Fig. 3c). However, whereas $FeO_T$ contents increase up through the Upper Zone, V drops off smoothly upwards. This rapid decrease in V is probably due to stripping of the V from the magma owing to crystallization of magnetite. As with both $TiO_2$ and $FeO_T$, there is a

**Table 1**: Representative whole-rock geochemical analyses of Skaergaard rocks

| Sample ID: | 210.9 | 648.4 | 90-22 | 474878-81 | 474823-26 | 474747-50 | 458.287 | 458.279 | 458.203 | 458.226 | 458.211 |
|---|---|---|---|---|---|---|---|---|---|---|---|
| Strat. (m): | 1881 | 1443 | 969·1, 1122·7 | 1091·4 | 1077·7 | 1058·9 | 875·0 | 752·0 | 558·0 | 294·0 | 7·0 |
| Unit: | UZb | UZa | MZ | MZ | MZ | MZ | LZc | LZc | LZb | LZb | LZa |
| *wt %* | | | | | | | | | | | |
| $SiO_2$ | 43·58 | 44·89 | 46·36 | 42·88 | 47·44 | 37·57 | 37·28 | 46·32 | 50·18 | 49·87 | 48·16 |
| $TiO_2$ | 3·31 | 5·31 | 5·10 | 8·58 | 5·32 | 10·36 | 10·19 | 3·13 | 1·28 | 0·81 | 1·36 |
| $Al_2O_3$ | 11·86 | 11·83 | 14·13 | 16·09 | 16·42 | 11·22 | 11·50 | 14·43 | 16·30 | 17·63 | 16·91 |
| $FeO_T$ | 22·96 | 18·46 | 15·13 | 15·89 | 11·62 | 22·71 | 21·78 | 14·49 | 8·99 | 7·98 | 10·61 |
| MnO | 0·35 | 0·27 | 0·22 | 0·18 | 0·17 | 0·25 | 0·25 | 0·20 | 0·17 | 0·14 | 0·17 |
| MgO | 2·4 | 5·59 | 5·19 | 3·38 | 4·08 | 5·42 | 5·93 | 6·44 | 7·23 | 7·96 | 9·01 |
| CaO | 8·83 | 9·67 | 9·86 | 8·62 | 9·88 | 8·66 | 9·36 | 11·25 | 12·31 | 12·50 | 10·52 |
| $Na_2O$ | 3·20 | 2·73 | 3·01 | 3·40 | 3·48 | 2·23 | 2·04 | 2·60 | 2·66 | 2·57 | 2·41 |
| $K_2O$ | 0·4 | 0·19 | 0·20 | 0·19 | 0·20 | 0·11 | 0·10 | 0·18 | 0·16 | 0·16 | 0·24 |
| $P_2O_5$ | 1·49 | 0·04 | 0·07 | 0·04 | 0·05 | 0·02 | 0·02 | 0·06 | 0·05 | 0·05 | 0·13 |
| *ppm* | | | | | | | | | | | |
| Ni | n.d. | n.d. | n.a. | 24 | 18 | 44 | 105 | 89 | 84 | 116 | 195 |
| Cu | 785 | 918 | 420 | 152 | 113 | 165 | 87 | 91 | 69 | 68 | 131 |
| V | 37 | 221 | 607 | 938 | 500 | 1490 | 2020 | 1320 | 287 | 197 | 191 |
| S | 100 | 300 | 200 | 100 | 100 | 42 | 20 | n.d. | n.d. | n.d. | n.d. |
| *ppb* | | | | | | | | | | | |
| Au | 0·71 | 1·88 | 33·3 | 117·0 | 225·0 | 66·0 | 1·62 | 1·52 | 1·26 | 1·76 | 2·30 |
| Ir | n.d. | n.d. | n.d. | n.a. | n.a. | n.a. | n.d. | n.d. | n.d. | n.d. | 0·15 |
| Pd | n.d. | 1·54 | 22·8 | 501·0 | 980 | 2680 | 44·4 | 10·3 | 5·79 | 5·86 | 8·75 |
| Pt | 0·64 | 0·48 | 10·1 | 23·0 | 53·0 | 127·0 | 15·2 | 6·33 | 2·89 | 3·71 | 6·72 |
| Rh | n.d. | n.d. | n.d. | n.a. | n.a. | n.a. | 2·96 | 2·87 | 0·28 | 0·22 | 0·39 |
| Ru | n.d. | n.d. | 0·21 | n.a. | n.a. | n.a. | 0·13 | 0·13 | 0·41 | 0·32 | 0·42 |
| Se | 420 | 936 | 705 | 76·2 | 91·5 | 73·0 | 4·73 | 21·9 | 27·2 | 29·6 | 100·8 |
| Te | 5·38 | 6·10 | 21·7 | 45·0 | 19·3 | 16·9 | 4·82 | 3·47 | 3·37 | 2·80 | 3·72 |

Stat. (m) = stratigraphic height above base of Lower Zone a; n.d., not detected; n.a., not analysed.

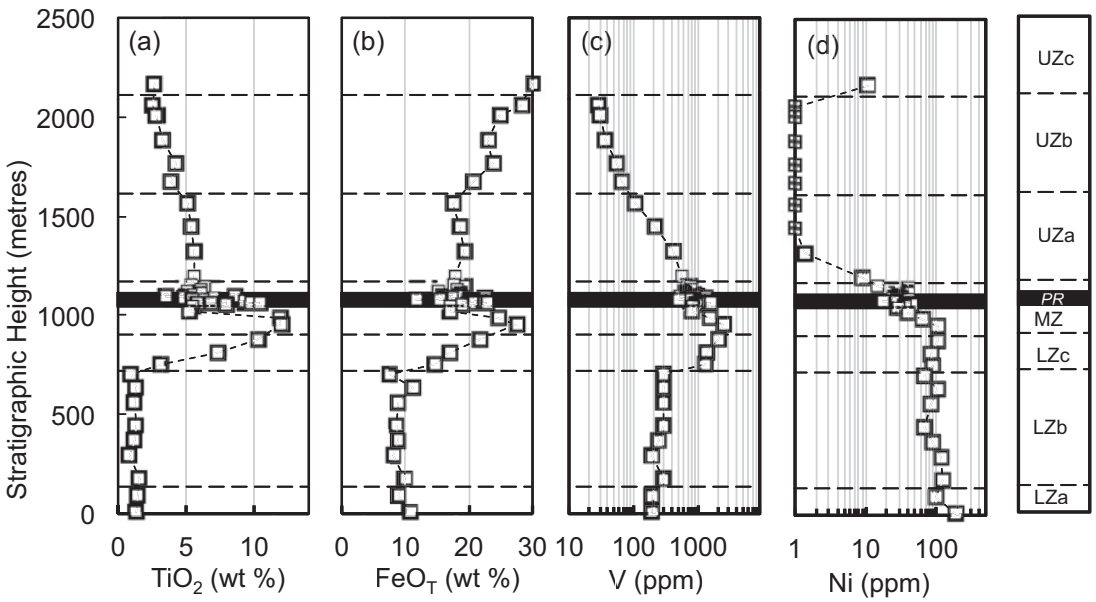


**Fig. 3.** Variations of $TiO_2$ (a), $FeO_T$ (b), V (c) and Ni (d) with stratigraphic height. It should be noted that $TiO_2$, $FeO_T$ and V increase rapidly through LZc and peak at 988 m; all three elements also exhibit a major trough at 1024 m, immediately below the Platinova Reef (PR). Abbreviations as in Fig. 1.

very sharp increase in V immediately above the base of LZc; the highest values are found in the interval up to 953 m, below the Reef package (Fig. 3c).

There is little variation in Ni content from the base of LZa to the top of LZc (Fig. 3d); Ni contents then drop rapidly through the MZ, approaching the level of detection for Ni toward the base of UZa (Fig. 3d).

The $P_2O_5$ contents of mafic cumulate rocks can be used to provide a measure of the fraction of trapped liquid in the cumulates provided no cumulus apatite is

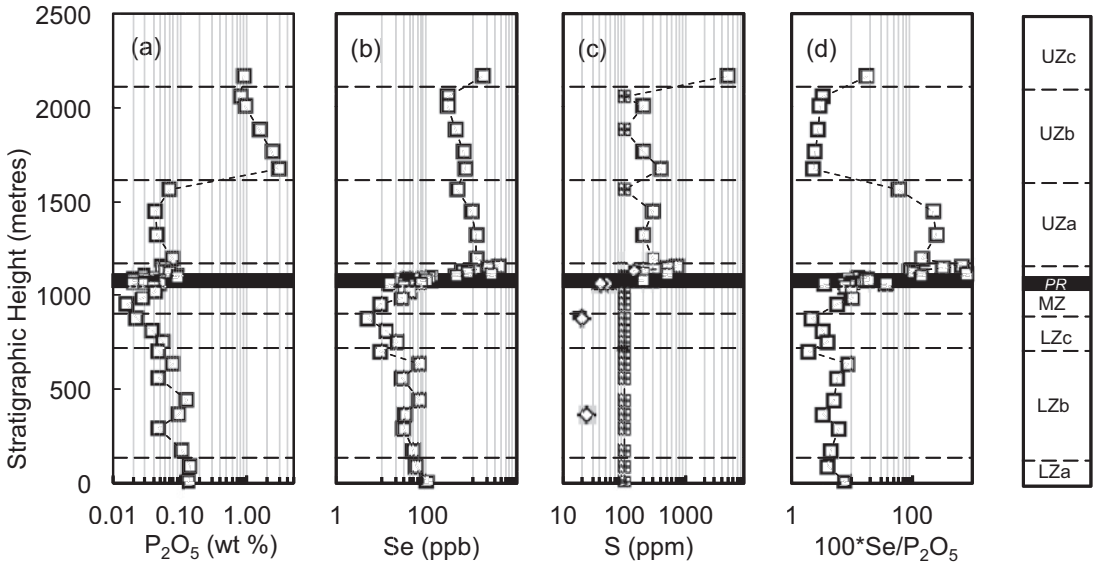


**Fig. 4.** Variations in $P_2O_5$ (a), Se (b), S (c) and Se/$P_2O_5$ (d) with stratigraphic height. Open squares, S determined by infra-red spectrometry; open squares with crosses, S is at the LoD (100 ppm S); open diamonds, S determined by mass spectrometry. Abbreviations as in Figs 1 and 2.

present (Tegner *et al.*, 2009). There is a gradual decline in $P_2O_5$ contents from 0·14 wt % at the base of LZa to 0·02 wt % at the base of the MZ (Fig. 4a); $P_2O_5$ values then increase up to the Reef package, although there are units within it that also have fairly low $P_2O_5$ contents (Tegner *et al.*, 2009). Above the Reef package, there is a slight increase in $P_2O_5$ contents to the top of UZa and then a sharp jump at 1671 m where the rocks contain 2·86 wt % $P_2O_5$ and define the base of UZb where cumulus apatite appears (Fig. 4a).

Selenium has a similar profile to that of $P_2O_5$ up to the level of the Reef package, decreasing from 101 ppb at the base of LZa to 4·7 ppb Se at the top of LZc; it then increases to the base of the Reef package and averages ~50 ppb within the lower part of the Reef showing Pd peaks. Selenium then increases to 121 ppb in the Au zone and then increases rapidly to reach a maximum of 3410 ppb above the Au zone at 1150 m (Fig. 4b; Table 1 and Supplementary Data Table 1). Selenium then gradually decreases upwards to 274 ppb at 2061 m (Fig. 4b).

None of the samples below the Reef package and only two of the samples from the Reef package have S contents above the limit of detection, LoD (100 ppm S) of the infra-red method (Fig. 4c). The samples above the Reef package generally have much higher S contents with a maximum of 7000 ppm, although three of these samples have S contents below the LoD. The S contents determined by the mass spectrometry technique range from 20 to 152 ppm (Table 1 and Supplementary Data Table 1; Fig. 4c); the two samples from below the Reef package have 20 and 24 ppm S. The sample immediately above the Reef package has 152 ppm S. Of particular note is that the sample from the main Pd peak (Pd5) with 2675 ppb Pd contains only 42 ppm S (Table 1 and Supplementary Data Table 1).

Figure 4d shows that there is a slight increase in Se/$P_2O_5$ ratio through LZb, followed by a slight drop in LZc; Se/$P_2O_5$ ratios climb steeply through the MZ and peak at the base of UZa.

The lowermost sample in LZa has 8·8 ppb Pd, 6·7 ppb Pt and 2·3 ppb Au (Fig. 5). However, whereas Pd and Au contents decrease only slightly up to the top of LZb, Pt contents decrease by a factor of ~5 to 1·5 ppb. Both Pd and Au then increase upwards through LZc and MZ towards the Pd Reef, except for a sharp drop at 1024 m, just below the mineralized zone; Pt exhibits an initial increase and then remains constant. The Au peaks at 1099·3 m (2800 ppb) and 1101·4 m (1990 ppb) occur above the main Pd peak (2675 ppb) at 1058·9 m; the Pt peak (149 ppb) occurs at 1060 m. All three metals decrease sharply above the mineralized zone; however, whereas Pd and Au eventually drop to their LoD, Pt first sharply decreases with stratigraphic height, and then exhibits a sharp increase above 1768 m (Fig. 5b).

Tellurium contents vary from 2·3 to 239 ppb, with the position of the Te peak at 1101·4 m corresponding to that of the Au peaks at 1099·3 m and 1101·4 m (Fig. 5d). The Te content of the sample at the Pd peak at 1058·9 m is 16·9 ppb, whereas that of the Pt peak at 1060 m is 8·9 ppb. The Te contents of the rocks above the Platinova Reef are only marginally higher than those below the Reef (Fig. 5d).

The bulk of the samples have extremely low Ir contents; only three of the samples, all from the lower part of the stratigraphic reference section, have Ir contents above the LoD (0·04 ppb; Table 1 and Supplementary Data Table 1). The sample with the highest Pd content (3210 ppb Pd) from the main Pd peak has an Ir content below the LoD. Ruthenium has a very similar distribution pattern to that of Pd in LZa and LZb (Table 1 and

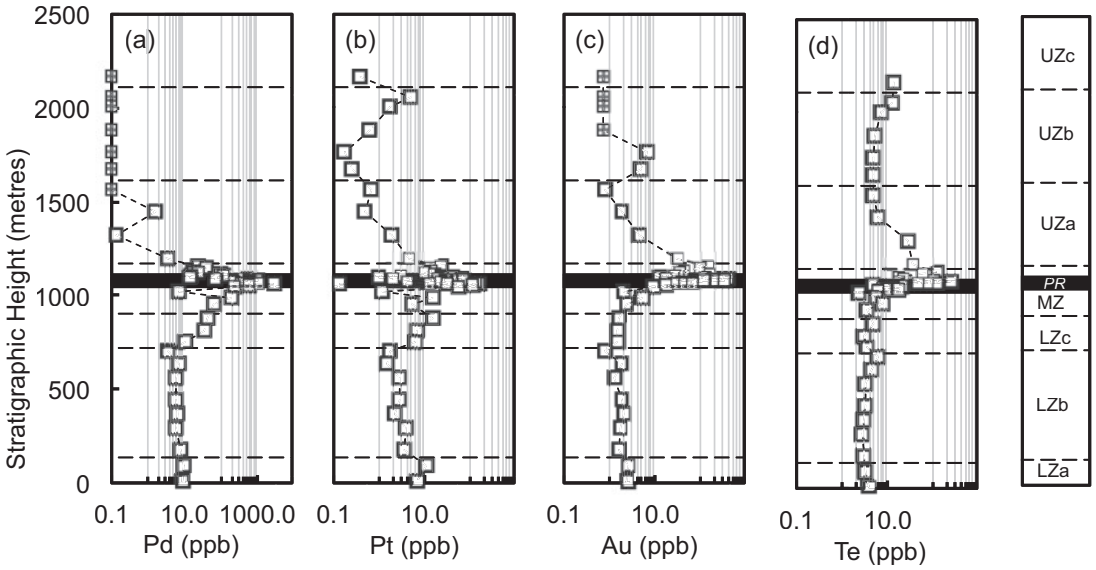


**Fig. 5.** Variations in Pd (a), Pt (b), Au (c), and Te (d) with stratigraphic height. It should be noted that all four elements increase sharply from the base of LZc upwards to the Platinova Reef (PR) with the exception of the reversal at 1024 m. Open squares with crosses, Pd and Au are at LoD. Abbreviations as in Figs 1 and 2.

Supplementary Data Table 1). However, whereas Pd increases through LZc, Ru drops to concentrations less than the LoD for Ru (= 0·13 ppb). Although the sample from the main Pd peak has a Ru content below the LoD, the three samples immediately above the Platinova Reef have Ru contents above the LoD for Ru (Supplementary Data Table 1); Ru values then drop below the LoD above this level. Rhodium exhibits a similar distribution pattern to that of Pd, extending from the base of the stratigraphic section to a stratigraphic height of 752 m (Supplementary Data Table 1). However, Rh exhibits a prominent peak below the Platinova Reef, between 742 and 875 m. Although the Rh contents of all samples above the Platinova Reef are below the LoD of 0·08 ppb Rh, our sample from the main Pd peak has 1·25 ppb Rh.

There is a narrow range in Cu (from 58 to 141 ppm) throughout the LZ and the MZ below the Platinova Reef; although there is a slight increase in Cu in the main Pd peak of the Platinova Reef, Cu values within the Reef up to the Au zone are in general only marginally higher than in the rocks below it (Fig. 6a; Supplementary Data Table 1). Copper contents increase rapidly from 122 ppm just below the Au peaks to 1240 ppm 11 m above the Reef (Fig. 6a; Supplementary Data Table 1). With the exception of a few reversals, Cu contents then continue to increase to a peak of 1969 ppm at 1150 m, ~50 m above the Au zone. With the exception of two samples, Cu contents remain above 650 ppm above the Cu peak.

There is a slight increase in $Cu/P_2O_5$ ratios from the base of LZa to the top of LZb (Fig. 6b); $Cu/P_2O_5$ ratios then increase rapidly through LZc and the lower part of the MZ up to 988 m, at which point they drop sharply to 1024 m just below the Reef, mimicking the patterns of both $TiO_2$ and $FeO_T$ (compare Fig. 6b with Fig. 3a and b). Above 1024 m, $Cu/P_2O_5$ ratios increase sharply to peak at the top of the Platinova Reef, above which ratios remain high until they drop sharply at 1615 m where apatite becomes a cumulus phase.

There is a slight decrease in Se/Te ratios from the base of LZa to the top of LZc, above which Se/Te ratios climb to the base of the Platinova Reef (Fig. 6c). With the exception of the Au zone, which has very low Se/Te ratios, Se/Te values within the Platinova Reef are lower than in the rocks above the Reef (Fig. 6c; Supplementary Data Table 1). Above the Au zone, there is a very rapid increase in Se/Te ratios, which remain elevated throughout the UZ (Fig. 6c).

There is little variation in Pd/Zr ratios from the base of LZa to the top of LZb (Fig. 7a); however, with the exception of a sharp reversal at 1024 m, there is a rapid increase in Pd/Zr ratios up to the Reef package. Within the Reef package, 1000 × Pd/Zr ratios vary widely, from 16 to 3060 (Supplementary Data Table 1); Pd/Zr ratios decrease very rapidly above the Reef Package, with most being <1 throughout the UZ (Fig. 7a). There is also very little variation in either Au/Zr or Cu/Zr ratios in LZa or LZb (Fig. 7b and c); however, both ratios increase upwards from the base of LZc to the Platinova Reef. The Cu/Zr peak is immediately above the Au peak, at the base of the Cu zone (Fig. 7c). Whereas Au/Zr ratios decrease upwards to UZc, there is only a minor upwards decrease in Cu/Zr ratios (Fig. 7b and c). Similar to Pd/Zr, Au/Zr and Cu/Zr ratios, Se/Zr ratios show very little variation in LZa and LZb; however, unlike the other ratios, Se/Zr ratios are lower in LZc than in LZa or LZb (Fig. 7d). There is a rapid increase upwards through the MZ and the Platinova Reef, with Se/Zr ratios reaching their maximum at the top of the MZ, immediately above the Au

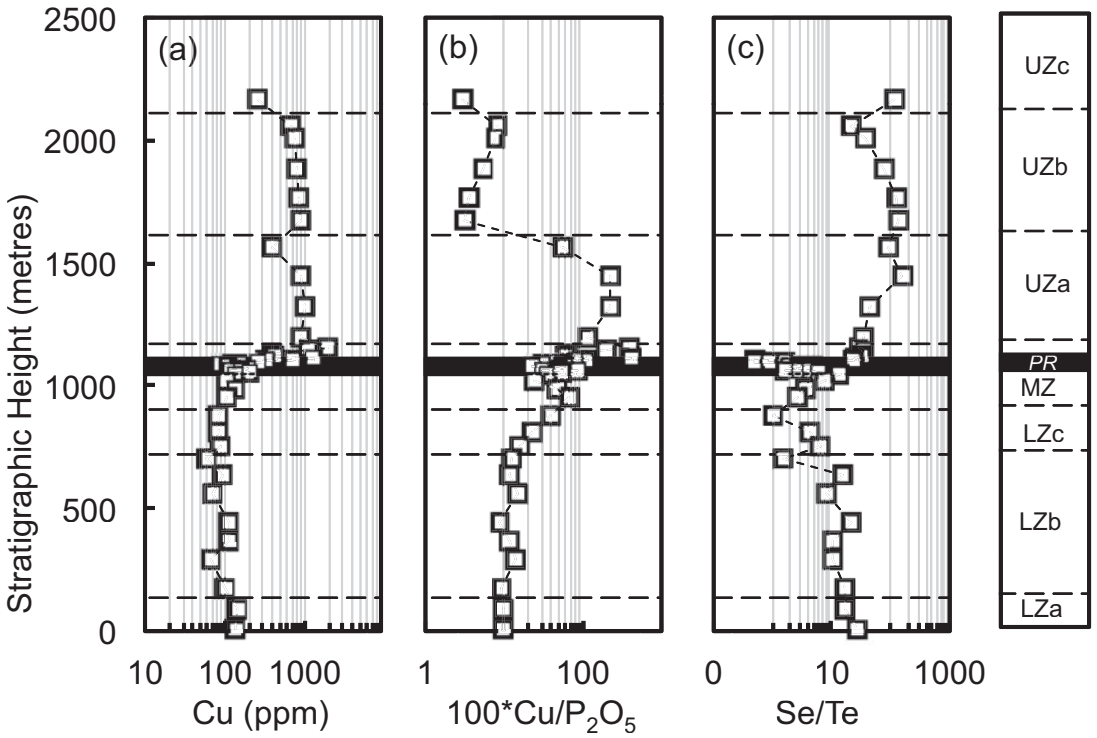


**Fig. 6.** Variations in Cu (a), $Cu/P_2O_5$ (b), and Se/Te (c) with stratigraphic height. It should be noted that although absolute Cu values increase only slightly from the base of LZc upwards, the significant increase in $Cu/P_2O_5$ indicates the presence of cumulus sulphides. Abbreviations as in Figs 1 and 2.

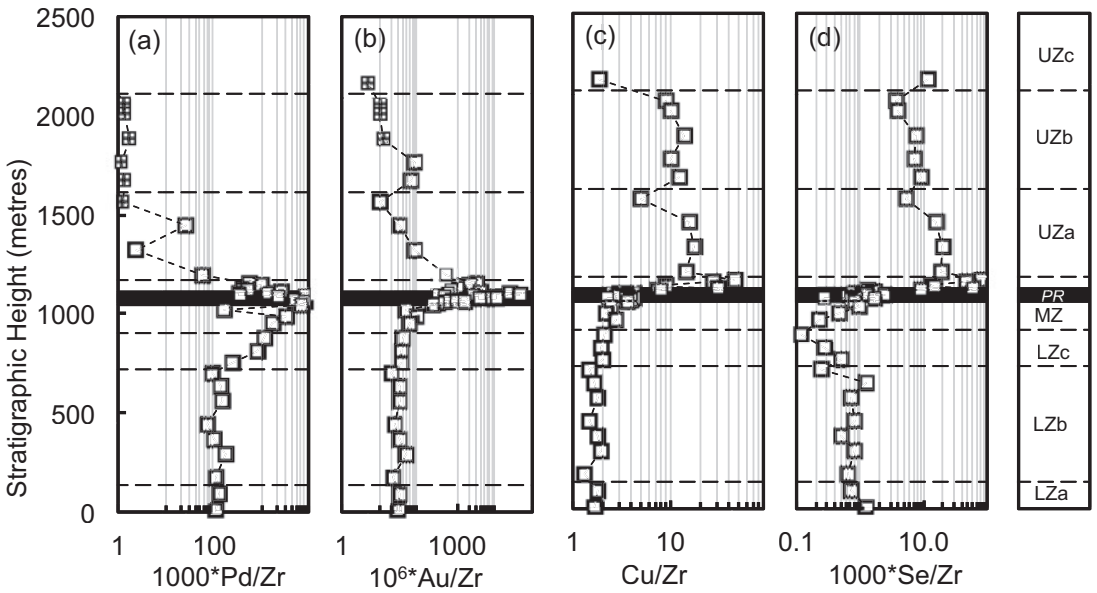


**Fig. 7.** Variations in Pd/Zr (a) Au/Zr (b), Cu/Zr (c) and Se/Zr (d) with stratigraphic height. The very rapid increase in Pd/Zr ratios from the base of LZc up to the Platinova Reef (PR), with the exception of the sharp reversal at 1024 m, should be noted. Open squares with crosses, samples are below LoD for Pd (a) or Au (b). Abbreviations as in Figs 1 and 2.

zone (Fig. 7d); there is then a gradual upwards decline in Se/Zr ratios in UZa and UZb.

Similar to both Cu/Zr and Pd/Zr ratios, Pd/Cu ratios are more or less constant in LZa and LZb (Fig. 8a); Pd/Cu ratios then increase rapidly upwards to the base of the Reef package, with the exception of a reversal at 1024 m. Within the Reef package, Pd/Cu ratios decrease sharply from the main Pd peak at 1058·9 m to the top of the Reef (Fig. 9b); Pd/Cu ratios decrease very rapidly above the Platinova Reef (Figs 8a and 9b). With the exception of a reversal at 1047·4 m, at the base of the Reef package, there is an upwards increase in Pd/Pt ratios from the base of LZa, where Pd/Pt ratios are ~1·0, to the main Pd peak at 1072·4 m where Pd/Pt = 59 (Fig. 8b).

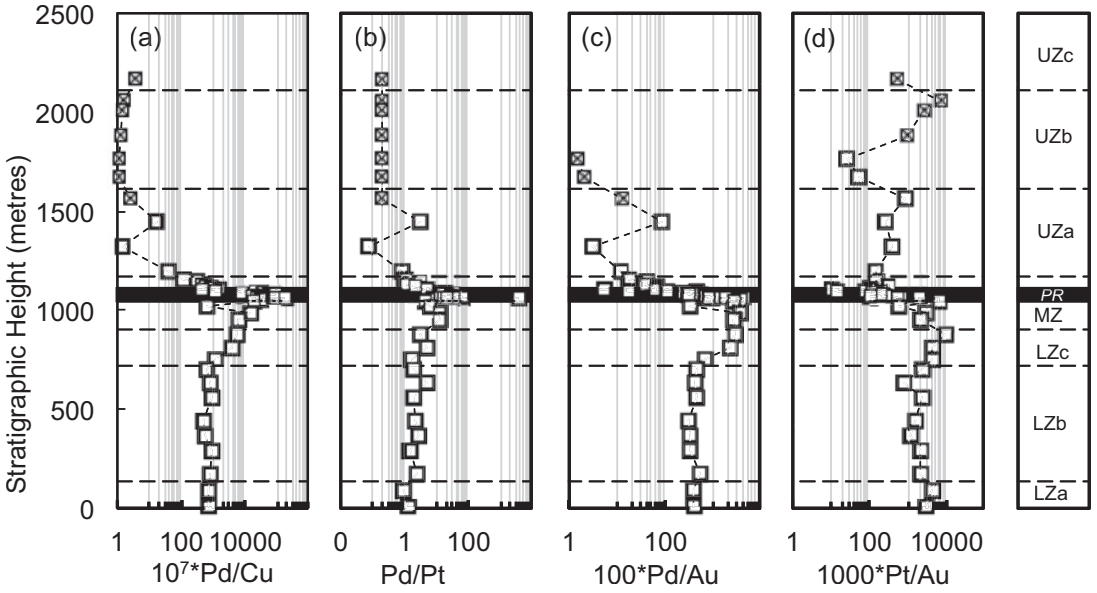


**Fig. 8.** Variations in Pd/Cu (a), Pd/Pt (b), Pd/Au (c) and Pt/Au (d) with stratigraphic height. The very sharp increase in Pd/Cu from the base of LZc up to the Platinova Reef (PR) should be noted. The sharp reversal in Pd/Pt ratio at 1024 m immediately below the Platinova Reef is a regional feature. Open squares with crosses, samples are below LoD for Pd (a, b) or Au (c, d). Abbreviations as in Figs 1 and 2.

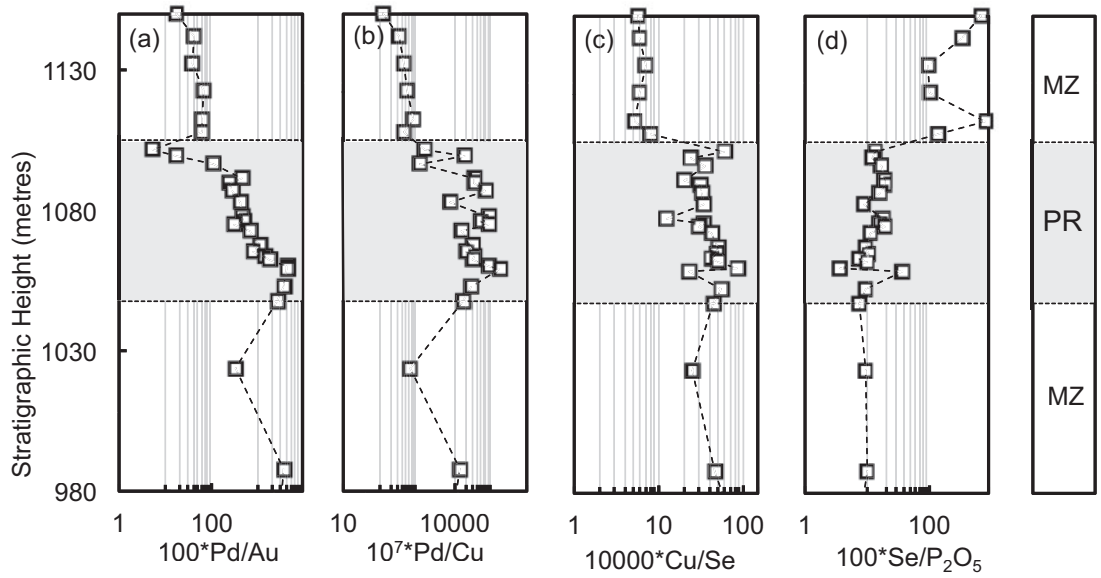


**Fig. 9.** Variations in Pd/Au (a), Pd/Cu (b), Cu/Se (c) and Se/$P_2O_5$ (d) ratios across the Platinova Reef. Abbreviations as in Figs 1 and 2.

Pd/Pt ratios then decrease rapidly through the upper portion of the Reef package and the overlying Upper Zone; Pd/Pt ratios above 1500 m are indeterminate because Pd values are below the LoD. The reversal in Pd/Pt at the base of the Reef package across the Skaergaard intrusion was also observed by Andersen *et al.* (1998). Variations in Pd/Au are similar to those of Pd/Cu with the exception that the increases in Pd/Au are not as great as those of Pd/Cu (Fig. 8c). There is a gradual decrease in Pt/Au from the base of LZa to the top of LZb, followed by an increase in Pt/Au through LZc (Fig. 8d); with the exception of a reversal at the main Pd peak, there is a decline in Pt/Au ratios through the MZ to just above the main Au peak (Fig. 8d, Table 1). There is a slight increase in Pt/Au through UZa, a sharp drop at the base of UZb, and then a sharp increase in Pt/Au through UZb (Fig. 8d).

As pointed out by Holwell & Keays (2014), there is a uniform decrease in Pd/Au ratios across the Platinova Reef (Fig. 9a). With the exception of the two samples from the Au zone at the top of Platinova Reef, there is a continuum in Pd/Au ratios from the base of the Platinova Reef to the base of the Cu zone at 1107·4 m (Fig. 9a). Although much more variable than the Pd/Au trend, there is also a decrease in Pd/Cu ratios across the Platinova Reef (Fig. 9b); however, the decrease in Pd/Cu

ratios is not nearly as large as that of Pd/Au. Whereas there is a slight decrease in Cu/Se ratios across the Platinova Reef, there is a slight increase in Se/$P_2O_5$ ratios (Fig. 9c and d).

The autolith at 900 m has higher $SiO_2$, $Al_2O_3$ and Se, but lower $TiO_2$, FeO, $Fe_2O_3$ and V, than the samples below (875 m) and above (953 m) it (Supplementary Data Table 1). The composition of the autolith is much more similar to the LZa and LZb samples than to samples higher in the stratigraphy; it is one of the few Skaergaard samples that have Ir contents above the LoD (Supplementary Data Table 1).

## DISCUSSION

### Magma chamber processes recorded by PGE geochemistry

It has been acknowledged by many researchers (e.g. Andersen *et al.*, 1998; Nielsen *et al.*, 2005; Andersen, 2006) that the Platinova Reef is the product of extreme fractionation of a ferrobasaltic magma. Andersen (2006) has argued that the Skaergaard magma became sulphide saturated at the level of the Platinova Reef and that all of the Cu, PGE and Au in the Reef were initially extracted from the Skaergaard magma in an immiscible magmatic sulphide melt. The present study has demonstrated that there is a rapid increase in the Pd contents of the Skaergaard rocks commencing ~300 m below the Platinova Reef (Fig. 5a); Pt also increases at this level, as does Au to a lesser extent (Fig. 5b and c). Andersen *et al.* (1998) found similar increases in Pd, Pt and Au in the footwall of the Platinova Reef. These increases in chalcophile metal content are decoupled from the lithophile trace elements as demonstrated by increasing Pd/Zr ratios from LZc upwards (Fig. 7a), and signal a major change in the chalcophile metal geochemistry of the Skaergaard magma well in advance of the main mineralization event (Fig. 5a). If an immiscible sulphide melt was the collector for the PGE and Au, why are the S contents of not only the Platinova Reef but also all of the Skaergaard rocks stratigraphically below the Reef so low? Was some other process responsible?

The 10-fold increase in both Se and Cu contents in the rocks lying above the Platinova Reef relative to their concentrations in the rocks below the Platinova Reef (Figs 4b and 6a) strongly suggests that the rate of production of magmatic sulphides above the Reef was much greater than that below the Reef. We will argue that sulphide saturation of the Skaergaard magma was initially limited to a boundary layer between the magma and a crystal mush and that the magma did not become fully sulphide saturated until the start of formation of the Cu Zone.

### Modelling the variation of the chalcophile metals in the Skaergaard intrusion

As discussed by other researchers including Nielsen *et al.* (2005), the Skaergaard magma had undergone a very significant amount of differentiation (~70%) by the time the Platinova Reef was formed.

The factors controlling the distribution of the metals throughout the Skaergaard intrusion can be modelled using the Rayleigh fractionation law:

$$C_L = C_O F^{(D-1)}$$

where $C_O$ is the initial concentration of the element, $F$ is the fraction of melt remaining, $C_L$ is the concentration of the element in the remaining melt, and $D$ is the mineral/melt partition coefficient for the element. Because the Skaergaard rocks are all cumulates with variable amounts of trapped melt, it is necessary to estimate the amount of trapped melt in each of our samples.

Sulphur, Se, Pd, Au, Cu and $P_2O_5$ are highly incompatible elements in the silicate phases and therefore accumulate in the residual melt of fractionating magmas until such times as the magma becomes saturated in phases that host these elements. In the case of S and Se that phase is a sulphide, whereas in the case of $P_2O_5$ it is apatite. The amounts of $P_2O_5$, S and Se in cumulate rocks prior to saturation in one of the host phases of these elements are therefore measures of the amount of trapped melt in the cumulates.

Tegner *et al.* (2009) estimated the trapped liquid contents of the Skaergaard cumulates from their $P_2O_5$, U and Rb contents; in general, they obtained excellent agreement between all three elements. To model the fractionation of metals during crystallization of the Skaergaard magma we use estimates of the fraction of trapped liquid in each of our samples based on their $P_2O_5$ contents and the equations developed by Tegner *et al.* (2009). Because apatite becomes a cumulus phase at a relative stratigraphic height of 1671 m, we used U contents rather than $P_2O_5$ above this level. The trapped melt fractions so calculated were reported by Tegner *et al.* (2009) and are also listed in Supplementary Data Table 1.

Assuming that all the Pd in a rock was contributed by its trapped melt content, then the Pd content of the melt is given by the Pd content of the rock divided by the amount of trapped melt in the rock. The hypothetical Pd contents of the trapped melts so calculated are plotted against the fraction of liquid remaining ($F$) for each sample in Fig. 10a; the hypothetical Au, Cu and Se contents of the trapped melt are calculated similarly and given in Fig. 10b, c and d, respectively.

Alternatively, the evolution of the melt can be estimated using the Rayleigh fractionation law. To do this the bulk partition coefficients (= concentration of elements in the solids/concentration of elements in the silicate melt) of Cu, Au, Se and Te were taken as zero; in contrast, Pd and Pt were assigned $D$ values of 0·4 and 1·0, respectively (Momme *et al.*, 2002). It was assumed that the Skaergaard intrusion crystallized from a single magma batch as a closed system (e.g. Wager & Brown, 1968). It was also assumed that the lowermost sample in our reference section had formed at $F = 0{\cdot}764$ (Tegner *et al.*, 2009). The concentrations of each

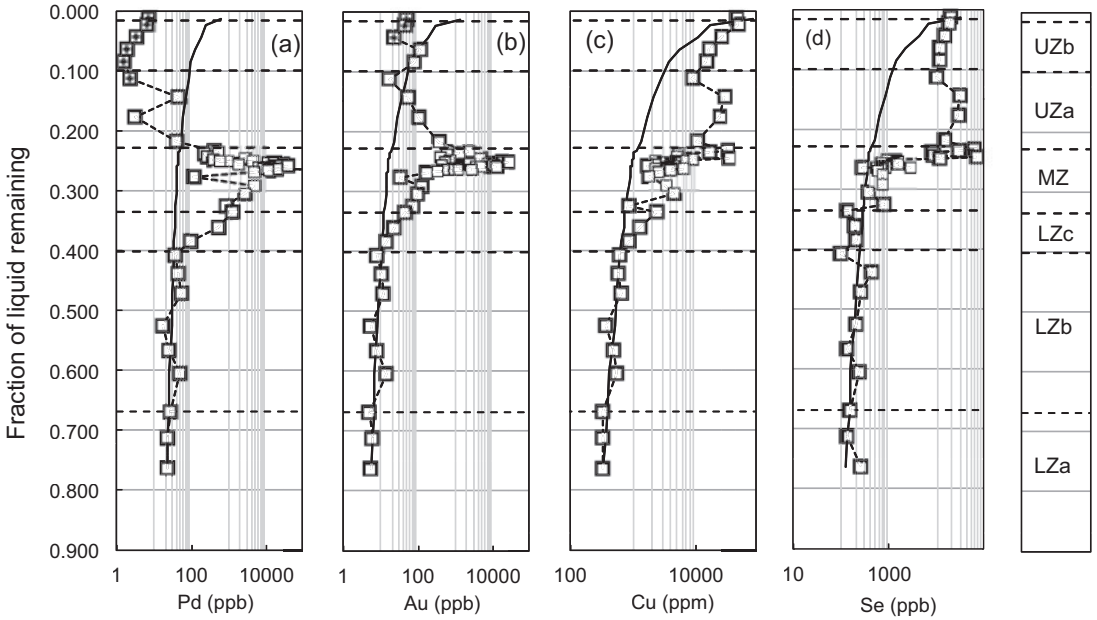


**Fig. 10.** Variations of Pd (a), Au (b), Cu (c) and Se (d) in hypothetical Skaergaard liquids (open squares) calculated from the bulk-rock compositions assuming their concentrations can be ascribed to the trapped liquid fraction (see text) plotted versus the fraction of liquid remaining. Open squares with crosses, samples for which Pd and Au are below LoD. The continuous curves represent model melts produced by Rayleigh fractionation. It should be noted that the hypothetical melt concentrations of all elements depart from the Rayleigh fractionation model curve at $F$ values = 0.407.

element in the initial liquid of the model melt were derived by an iterative process in which the model melt was fitted against the hypothetical melt composition calculated from the bulk composition of the cumulate rocks (i.e. the concentration in the sample divided by the fraction of trapped melt) in a plot of element concentration against $F$ (Fig. 10). This fit was made for those samples in LZa, LZb and LZc without elevated Pd, Cu, Au and Se contents; that is, for samples that occur below a stratigraphic height of 752 m at which $F$ is less than 0·4.

For Pd, there is a good fit between the Rayleigh fractionation model curve and the composition of the hypothetical melt from $F = 0{\cdot}764$ to $F = 0{\cdot}407$ (Fig. 10). This is interpreted to mean that all the Pd in the samples can be explained by the trapped liquid content. However, the curve for the hypothetical melt composition begins to deviate from the model melt at $F = 0{\cdot}385$; this corresponds to a relative stratigraphic height of 752 m, at which position there is a sharp increase in Pd (Fig. 5). The increase in the Pd content of the hypothetical melt relative to the Rayleigh fractionation model curve is interpreted to be caused by the presence of a non-silicate, non-oxide phase in the samples. It will be shown below that this phase was an immiscible sulphide liquid.

Plots of Cu and Au are very similar to the Pd plot (Fig. 10b and c). The simplest way to interpret these graphs is that prior to the deviation of the hypothetical melt curve away from the fractionation curve, all of the Pd, Cu and Au in the rocks was contributed by the trapped liquid. Although not shown, similar plots constructed for Pt and Te deviate away from the Rayleigh fractionation model curves at the same $F$ value. There is, however, considerable scatter in both the measured and calculated Pt values.

The stage at which the Skaergaard magma became saturated in a PGE-rich cumulus phase is defined by the point at which Pd deviates away from the Rayleigh fractionation model liquid curve at $F = 0{\cdot}385$ or 752 m, which is at the base of LZc. This point is ~300 m below the Pd peak in the mineralized zone at 1053 m (Fig. 5a).

## Sulphide saturation induced by changes in major element chemistry

The capacity of silicate melts to dissolve reduced S increases with increasing temperature and FeO content but decreases with pressure and $fO_2$ (Haughton *et al.*, 1974; O'Neill & Mavrogenes, 2002). The S capacities of magmas are also influenced by their chemical compositions other than FeO, including $H_2O$ contents.

Prior to sulphide saturation of the Skaergaard magma, Pd, Au, Cu and S would have built up in the residual melt by fractionation because they are all incompatible elements in sulphide-undersaturated magmas and mimic the incompatible lithophile trace elements. Although some FeO would have been removed in the mafic minerals (e.g. olivine, clinopyroxene) crystallizing from the magma, FeO would have built up along with S in the residual melt (Brooks & Nielsen, 1978). However, once Fe–Ti oxides started to crystallize the rate of build-up of FeO in the residual magma would have slowed (e.g. Tegner & Cawthorn, 2010) or reversed (Hunter & Sparks, 1987). As the temperature of the Skaergaard

magma dropped from ~1140°C at the base of LZa to ~1100°C at the base of LZc (Thy *et al.*, 2009*b*), the combined effect of near-stagnant FeO content and decreasing temperature could have driven the magma to S saturation as a consequence of the formation of cumulus Fe–Ti oxides.

The S content of the Skaergaard magma at sulphide saturation (SCSS) can be calculated using the melt compositions given by Tegner & Cawthorn (2010) and the following equation from Li & Ripley (2009):

$$\ln S = -1{\cdot}76 - 0{\cdot}474(104/T) - 0{\cdot}021P + 5{\cdot}559X\mathrm{FeO} + 2{\cdot}565X\mathrm{TiO_2} + 2{\cdot}709X\mathrm{CaO} - 3{\cdot}192X\mathrm{SiO_2} - 3{\cdot}049X\mathrm{H_2O}$$

where $T$ is temperature in Kelvin and $P$ is pressure in kilobars. The temperature of the Skaergaard magma at $F = 0{\cdot}407$ was 1100°C, its $H_2O$ content was 0·25 wt % and the pressure was 1·3 kbar (Thy *et al.*, 2009*b*). At $F = 0{\cdot}407$ the Skaergaard magma contained 45·60 wt % $SiO_2$, 17·53 wt % FeO, 5·08 wt % $TiO_2$ and 9·19 wt % CaO (Tegner & Cawthorn, 2010). At these conditions, the Li *et al.* (2009) equation predicts that the S content of the Skaergaard magma at sulphide saturation was 1865 ppm S. The fraction of trapped melt in the sample at $F = 0{\cdot}407$ is 0·094. Hence, the trapped melt, with 1865 ppm S, would contribute 175 ppm S to the rock. However, the S content of the sample at 710 m is below the 100 ppm detection limit of the infra-red method (Fig. 4c). The S contents measured by mass spectrometry of the samples below and above the sample at 710 m are 20 and 24 ppm, respectively, with an average of 22 ppm S. Assuming that the sample at 710 m also has 22 ppm S and not 175 ppm S as predicted by the Li *et al.* (2009) S capacity equation, this suggests either that there has been significant post-magmatic S loss from this sample as advocated by Andersen (2006) or that the Skaergaard magma did not become sulphide saturated at the base of LZc as a result of changes in its physical and chemical properties that are accommodated in the Li *et al.* (2009) equation.

## Oxidation as a driver of sulphide saturation

The rapid increases in $FeO_T$, $TiO_2$ and V commencing at the base of LZc mark the point in the Skaergaard stratigraphy at which cumulus Fe–Ti oxides began to form in addition to intercumulus Fe–Ti oxides between the cumulus silicate phases. By removing $Fe^{3+}$ from the magma, the formation of cumulus magnetite ($FeO.Fe_2O_3$) would have decreased the $fO_2$ of the magma. In addition, the crystallization of cumulus magnetite and ilmenite would have slowed down the build-up of both FeO and $TiO_2$ in the residual liquid and hence brought the magma closer to the sulphide saturation surface as indicated by the Li *et al.* (2009) equation.

The Skaergaard magma is inferred to have followed an iron-rich liquid line of descent (Brooks & Nielsen, 1978; Brooks *et al.*, 1991; Tegner, 1997; Tegner & Cawthorn, 2010) under a low oxygen fugacity regime (Morse *et al.*, 1980; Sato & Valenza, 1980). Under these conditions the S in the magma would have been distributed according to the following equation suggested by Jugo *et al.* (2005):

$$S^{2-}\mathrm{melt} + 2O_2 \leftrightarrow {SO_4}^{2-}\mathrm{melt}.$$

The relative amounts of $S^{2-}$ and $S^{6+}$ in the magma would have been controlled by the $fO_2$ of the magma (Jugo *et al.*, 2010), which in turn would have been controlled by the $Fe^{3+}/Fe^{2+}$ ratio of the magma. Although McBirney (1996) argued that there was a steady decrease in the $fO_2$ of the Skaergaard magma from the base of LZa to UZa, there must have been changes in the gradient of decreasing $fO_2$ as different phases hosting $Fe^{2+}$ and $Fe^{3+}$ came onto the liquidus. Up to LZc, olivine and clinopyroxene were both crystallizing from the magma and hence removing $Fe^{2+}$; as a result, the $Fe^{3+}/Fe^{2+}$ ratio of the magma would have increased with differentiation (Morse *et al.*, 1980; Toplis & Carroll, 1996; Thy *et al.*, 2009*a*). However, in LZc, magnetite became a liquidus phase and this would have caused a drop in the $fO_2$ of the magma (Morse *et al.*, 1980; Frost & Lindsley 1992; Toplis & Carroll, 1996; Thy *et al.*, 2009*a*). As a result of the decrease in $fO_2$, the ratio of $S^{6+}/S^{2-}$ would have decreased and more of the total S in the magma was $S^{2-}$; because total S was continuing to build up in the magma owing to magmatic differentiation, there would have been a sharp increase in the $S^{2-}$ content of the magma as a result of the appearance of cumulus magnetite.

The formation of magnetite would have removed both ferrous and ferric iron as well as $O_2$ from the magma and as a result destabilized some of the ${SO_4}^{2-}$ in the magma, converting it into $S^{2-}$, which is much less soluble in magmas than ${SO_4}^{2-}$ (Jugo *et al.*, 2005). Because the formation of magnetite was a gradual process that continued with differentiation of the Skaergaard magma, the production of $S^{2-}$ was also a gradual process.

Jenner *et al.* (2010) have described a similar situation during the differentiation of island arc basalts, during which FeO builds up in the magma until such time as magnetite began to crystallize; as a result, the magma becomes sulphide saturated owing to the reduction of sulphate to sulphide. Jenner *et al.* (2010) inferred the presence of Cu-rich sulphides in arc basalts that they interpreted to be bornite, which, together with chalcocite, is the major sulphide phase in the Platinova Reef.

Although the conversion of S from sulphate to sulphide species probably played a significant role in increasing the reduced S content of the Skaergaard magma, this cannot have been the sole explanation for the dramatic increases in Pd, Pt, Au and Cu beginning at the base of LZc. This is because regardless of the initial speciation of S in the Skaergaard magma, the magma would have become sulphide saturated when its reduced S content reached 1865 ppm.

## Saturation in Cu-sulphides

The rapid increase in Pd above the base of LZc suggests that Pd, along with Pt and Au, began to segregate in some type of cumulus phase. It will be shown below that this cumulus phase was a Cu–PGE-rich sulphide melt.

Much of the Pd in the Platinova Reef is present as Pd–Cu alloys, such as skaergaardite, PdCu (Rudashevsky *et al.*, 2004) and nielsenite, $Pd_3Cu$ (McDonald *et al.*, 2008). Experimental studies indicate that the solubilities of Pd and Pt in sulphide-free basic silicate melts at 1450°C are 390 ppm and 8·9 ppm, respectively (Borisov & Danyushevsky, 2011); hence, it is unlikely that Pd and Pt had exceeded their solubility limits and segregated from the magma as alloys. The intimate association between the Pd–Cu alloys in the Platinova Reef and Cu-sulphides (Rudashevsky *et al.*, 2004; McDonald *et al.*, 2008) strongly suggests that the Pd (and other PGE) segregated from the magma as PGE-rich sulphides. We suggest that the boundary layer of the Skaergaard magma became sulphide saturated at the base of LZc and that Pd was removed in the PGE-rich cumulus sulphides that segregated from the magma. Although there is very little change in the absolute Cu contents of the Skaergaard rocks (Fig. 6a), there are significant increases in $Cu/P_2O_5$ and Cu/Zr through LZc (Figs 6b and 7c). As Cu and Zr are highly incompatible elements in sulphide-undersaturated silicate melts, they accumulate in the residual melt during magmatic differentiation. However, once the melt becomes sulphide saturated and immiscible magmatic sulphides segregate from the melt, there are rapid decreases in both $Cu/P_2O_5$ and Cu/Zr ratios; in the case of the cumulus rocks of the Skaergaard intrusion, the increases in $Cu/P_2O_5$ and Cu/Zr ratios indicate the presence of Cu-bearing magmatic sulphides. The fractionation of $Cu/P_2O_5$ and Cu/Zr cannot be an effect of trapped liquid crystallization. Given that the rocks in this stratigraphic interval are essentially adcumulates with less than 5% trapped liquid on average (Tegner *et al.*, 2009), we therefore interpret the increase in Cu/Zr as an effect of cumulus Cu-bearing sulphide. The much greater increase in Pd/Zr ratios than Cu/Zr ratios (Fig. 7) is simply a reflection of the much larger sulphide melt/silicate melt partition coefficients ($D$) for Pd than for Cu; Mungall & Brenan (2014) reported from sulphide–silicate partitioning experiments conducted at log $fO_2 = -9{\cdot}58$ that $D_{Pd} = 2{\cdot}15 \times 10^5$ whereas $D_{Cu} = 1{\cdot}45 \times 10^3$. These experimental partition coefficients are in accordance with those ($D_{Pd} = 35\,000$, $D_{Cu} = 1380$) reported by Peach *et al.* (1990) from a study of sulphide blebs in MORB glasses.

Ripley *et al.* (2002) demonstrated that the S contents of magmas at sulphide saturation decrease significantly with increasing Cu content and with increasing Cu/Fe ratios of the sulphide melt segregating from the magma. Although the FeO contents of the silicate melts in the experimental charges used by Ripley *et al.* (2002) were lower than those estimated by Tegner & Cawthorn (2010) for the Skaergaard melt when it reached sulphide saturation at the base of LZc (~6 wt % FeO vs ~20 wt % FeO, respectively), we argue that the experimental results are applicable to Skaergaard because the sulphide phases in the experiments are also observed in Skaergaard. Therefore, knowing the Cu/Fe ratio of the sulphide melt that segregated from the Skaergaard magma can provide an estimate of the S content of the magma when it became sulphide saturated. As discussed below, it is highly probable that there was only minimal if any S loss from the Skaergaard rocks and that the original sulphides in the cumulate rocks below the Platinova Reef were the same as those in the Reef. The major sulphide minerals in the Reef are bornite ($Cu_5FeS_4$), with lesser amounts of chalcocite ($Cu_2S$) and digenite ($Cu_9S_5$), and minor chalcopyrite ($CuFeS_2$) (Rudashevsky *et al.*, 2004). Assuming equal proportions of bornite and chalcocite–digenite, the average Cu:Fe ratio of the sulphides would be 12:1. The experimental data of Ripley *et al.* (2002) predict that for sulphides with Cu:Fe = 12, the S content of the Skaergaard magma would have been ~120 ppm at sulphide saturation. This is more than an order of magnitude less than the S content of the magma at sulphide saturation estimated from the Li & Ripley (2009) equation based on the major element composition of the rocks.

## Initial chalcophile element content of Skaergaard magma

The initial chalcophile metal contents of the Skaergaard magma are the input values for the concentration of elements required to fit the Rayleigh law fractionation curves to the compositions of the LZa and LZb cumulates that formed prior to sulphide saturation. Hence, the parental Skaergaard magma is estimated to have contained 240 ppm Cu, 89 ppm S, 4·0 ppb Au, 9 ppb Pt, 18·7 ppb Pd, 90 ppb Se and 5·7 ppb Te. Previous estimates of the chalcophile metal content of the Skaergaard magma have been based on samples from the chilled margins of the intrusion (Table 2); these estimates vary considerably and are generally very different from the estimates obtained in this study. Nielsen (2004) estimated the Cu content of the Skaergaard parental magma to be 265 ppm using the bulk summation of the cumulate rocks; this value is similar to our estimate (240 ppm).

The S content of the Skaergaard magma predicted by our modelling (89 ppm) is only slightly lower than our S value for its chilled margin (100 ppm), but double the 47 ppm S reported by Wager *et al.* (1957) for the chilled margin (Table 2). The modelling suggests that the S/Se ratio of the Skaergaard magma was 937, whereas the chilled margin sample analysed gave a S/Se ratio of 1180 (Table 2); although similar to each other, these values are much lower than the S/Se ratio of the mantle (2560 ± 150; Dreibus *et al.*, 1995) but only

**Table 2**: Estimates of the chalcophile metal content of the initial Skaergaard magma

| | Cu (ppm) | S (ppm) | Ir (ppb) | Ru (ppb) | Rh (ppb) | Pt (ppb) | Pd (ppb) | Au (ppb) | Se (ppb) | Te (ppb) | Pd/Pt | S/Se | References |
|---|---|---|---|---|---|---|---|---|---|---|---|---|---|
| High-Ti plateau basalts* | 142 | | 0·22 | 0·5 | 0·3 | 5·3 | 5·9 | 9·5 | | | 1·13 | | Momme *et al.* (2006) |
| Low-Ti plateau basalts* | 184 | | 0·05 | 0·5 | 0·7 | 10·4 | 17·3 | 11·6 | | | 1·66 | | Momme *et al.* (2006) |
| SKD chill | | | | | | | | 7 | | | | | Vincent & Smales (1956) |
| SKD chill | | | | | | | 1·8 | | | | | | Vincent & Crocket (1960) |
| SKD chill | 108 | 47 | | | | | | | | | | | Wager *et al.* (1975) |
| SKD chill (GGU 366912) | | | | | | 23 | 53 | 45 | | | 2·30 | | Andersen *et al.* (1998) |
| SKD chill (GGU 366912) | 115 | | | | | 10 | 49 | 57 | | | 4·9 | | Nielsen & Brooks (1995) |
| SKD chill (GGU 366912) | 116 | | | | | 9 | 33·9 | 36 | | | 3·77 | | Momme (2000) |
| SKD magma | 265 | | | | | | | | | | | | Nielsen (2004) |
| SKD magma† | 250 | 894 | | | | | | | | | | | Andersen (2006) |
| SKD chill (GGU 366912) | | 100 | | | | | | | 84·6 | 6·7 | | 1180 | This study |
| SKD magma† | 240 | 89 | | | | 9 | 18·7 | 4 | 95 | 5·7 | 2·08 | 937 | This study |
| SKD (average LZa,b) | 99 | | <0·04 | 0·4 | 0·3 | 3·9 | 6·8 | 1·76 | | | 1·71 | | This study |
| SKD dyke (GGU 361036)‡ | 613 | 800 | | | | 6·7 | 16·4 | 15·1 | 344 | 21 | 2·45 | 2330 | This study |
| SKD dyke (GGU 361054)‡ | 162 | 200 | | | | 20·6 | 14·8 | 16·1 | 129 | 4·2 | 0·72 | 1550 | This study |

*Most primitive composition.
†Modelled Cu and S contents.
†Skaergaard-like dyke.

slightly higher than the S/Se ratio of one of the two Skaergaard-like dykes analysed (Table 2).

## Post-magmatic S loss?

An enigmatic feature of all of the mineralized samples in the Skaergaard intrusion is their very low S contents, with only one sample from the mineralized zone and none from the rocks below it having S contents above the detection level of the infra-red technique (100 ppm S). Although the five samples in which S was determined by mass spectrometry have measurable S contents, the sample from the main Pd peak has only 42 ppm S and the two samples below the Platinova Reef have S contents of 22 and 24 ppm. A significant question is whether or not the parental Skaergaard magma had a low S content. If it did not, then at what stage did the Skaergaard rocks lose their S?

Wohlgemuth-Ueberwasse *et al.* (2013) suggested that the high Cu/Fe ratios of the Skaergaard sulphides are due to oxidation at the magmatic stage; however, as the driving mechanism for sulphide saturation was the appearance of cumulus magnetite this appears unlikely, as the crystallization of magnetite would have reduced the $fO_2$ of the magma rather than increased it. Godel *et al.* (2014) argued that sulphides not completely enclosed in Fe–Ti oxides had undergone partial to complete dissolution during post-magmatic processes. However, in a more comprehensive study of sulphide textures in samples from the Platinova Reef, Holwell *et al.* (2015) concluded that there had been no significant hydrothermal S loss. Andersen *et al.* (1998) and Andersen (2006) have argued that the original sulphides in the Lower and Middle Zones of the Skaergaard intrusion were pyrrhotite–chalcopyrite assemblages that were oxidized and desulphurized during cooling of the crystalline rocks and replaced by bornite–chalcocite–magnetite assemblages; as a result, a significant amount of S was mobilized. Andersen (2006) also suggested that S leached from rocks below the Platinova Reef was added to the rocks above the Reef.

Selenium exhibits very strong geochemical coherence with S at high temperatures and substitutes in the S site in sulphides. From experimental studies, Yamamoto (1976) showed that S and Se are fractionated from each other during interaction of sulphides with hydrothermal fluids at temperatures less than 300°C, because whereas S may be leached by the fluids Se is inert. However, at temperatures above 300°C, S and Se behave in a very similar fashion. From leaching experiments in which pure $H_2O$ was allowed to interact with sulphide-bearing greywackes, Ewers (1977) showed that ~20% of the Se in the greywacke was leached at temperatures >300°C. Strong support for the existence of a fossil hydrothermal system in the Skaergaard intrusion is provided by the detailed oxygen isotope studies of Norton & Taylor (1979) and Taylor & Forester (1979). Norton & Taylor (1979) argued that at least 75% of the fluids that had interacted with the Skaergaard rocks had done so at temperatures >480°C. If these fluids had mobilized S they would also have mobilized Se. Because of the strong geochemical coherence between S and Se at elevated temperatures, Se can be used as a proxy for S: any high-temperature loss of S would also be recorded by a loss of Se. The excellent correlation between Se and $P_2O_5$ in the lower portion of the Skaergaard intrusion provides a strong case against any significant mobilization or loss of Se (and, hence S) from the Skaergaard rocks (Fig. 4d). Further evidence that there was no significant loss of Se (or S) is provided by the excellent fit between Se in the modelled Skaergaard liquid calculated from the Rayleigh fractionation law and the measured Se in the trapped liquid fraction of the cumulate rocks (Fig. 10d). The Se content of the initial parental Skaergaard melt (90 ppb) used in the modelling is almost identical to that of the chilled margin of the Skaergaard (86·4 and 82·1 ppb; Table 2). Although the Se/Zr ratios of some of the LZc samples are lower than those of the LZb samples (Fig. 7d), it is suggested that this does not indicate Se loss, but is rather due to the very low Se contents of

these rocks combined with the fact that the Zr in the samples is contributed by not only Zr in the trapped melt fraction but also by Zr in clinopyroxene. Although the S contents of the rocks in and below the Platinova Reef are below the detection limit (100 ppm) of the infra-red method used to measure S, estimates of their S contents can be made if it is assumed that all of the Cu and S in the rocks is hosted by sulphides. Rudashevsky *et al.* (2010) estimated that 58% of the sulphides in the mineralized zone consist of bornite ($Cu_5FeS_4$) alone or of bornite with chalcocite ($Cu_2S$) and that 42% consist of chalcocite only. They further demonstrated that the bornite contained an average of 63·0 wt % Cu and 24·5 wt % S, whereas the chalcocite had an average of 78·5 wt % Cu and 20·1 wt % S. Assuming that the sulphide assemblages consist of 80% bornite and 20% chalcocite, the average Cu and S concentrations of the sulphides in the mineralized zone are 72·3 wt % and 22·2 wt %, respectively. Hence, the S contents of the Skaergaard rocks within and below the Platinova Reef should be 22·2/72·3 times their Cu contents. The S contents of the Skaergaard rocks estimated from their Cu contents are given in Supplementary Data Table 1; the excellent agreement between the S content estimated this way and that measured by mass spectrometry confirms the validity of using Cu values to estimate the S contents of these samples.

The S contents of the Skaergaard rocks estimated from their Cu contents have been used along with the measured S and Se values to calculate S/Se ratios for all of the Skaergaard rocks. The variations in S/Se ratio as a function of stratigraphic height are given along with those of Pd/Se and Cu/Se in Fig. 11. All three ratios show little variation in LZa and LZb, but increase steeply through LZc, and then decrease from 875 m at the top of LZc to the base of the Platinova Reef (Fig. 11). With the exception of one S/Se data point, there is a rapid plunge in all three ratios immediately above the Platinova Reef package (Fig. 11); the lowest S/Se ratio (200) here is less than a tenth of the normal mantle S/Se ratio of 2500 ± 270 (Dreibus *et al.*, 1995). The lowest Cu/Se ratio (521) occurs immediately above the main Au peak at the top of the Reef package and at the base of the Cu zone. Both S/Se and Cu/Se ratios then climb rapidly towards the top of the stratigraphic section, whereas Pd/Se plummets sharply (Fig. 11). The dramatic decrease in Cu/Se ratios from 18 300 at 875 m to 521 at the base of the Cu zone is accompanied by a 510 times increase in Se contents, which increase from 4·7 to 2380 ppb over this same interval (Fig. 4b). This increase in Se is accompanied by significant decreases in $TiO_2$ and $FeO_T$ contents (Fig. 3).

The increases in S/Se (and Cu/Se) ratios upwards through LZc are due to two factors. Because Se has a high sulphide melt/silicate melt partition coefficient ($D_{Se} = 1770$; Peach *et al.*, 1990) the first cumulus sulphides to segregate from the magma had lower S/Se than sulphides that segregated later. Further, although

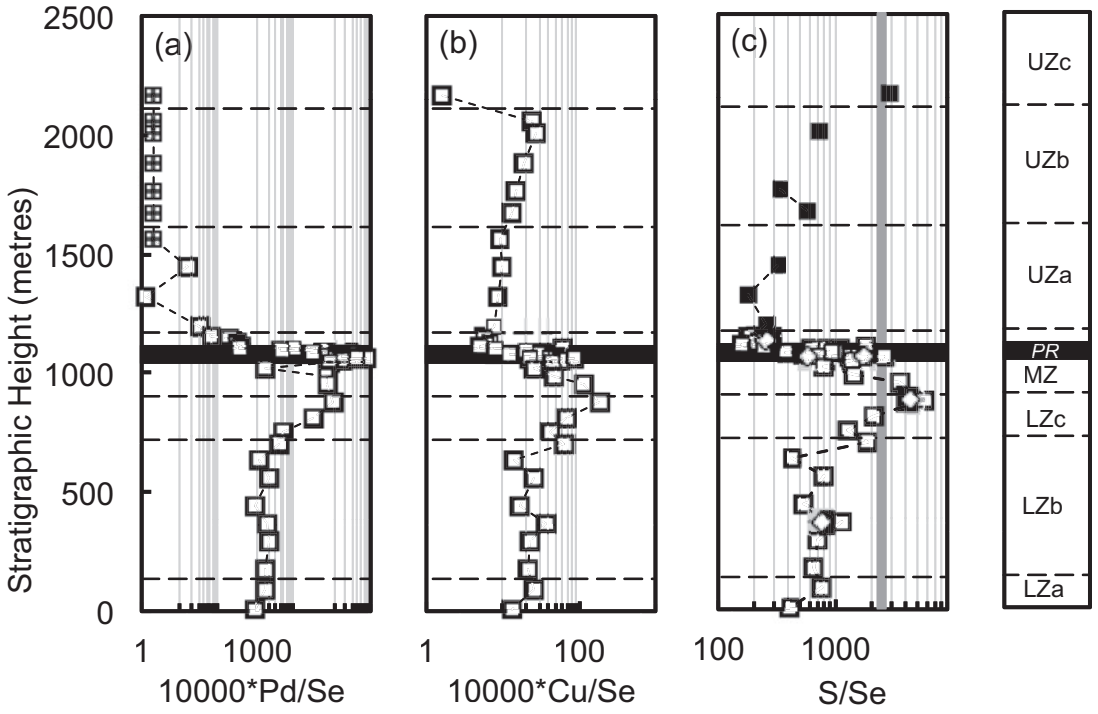


**Fig. 11.** Variations in Pd/Se (a), Cu/Se (b) and S/Se (c) with stratigraphic height. Filled squares, S contents of the samples determined by infra-red spectrometry; open squares, S contents of the samples calculated from the Cu contents of the samples; open diamonds, S contents of the samples determined by mass spectrometry; open squares with crosses, samples for which Pd is below LoD. The excellent agreement between the S/Se ratios in samples in which the S was calculated from Cu and those in which the S was determined by mass spectrometry should be noted. The grey vertical line in (d) is the S/Se ratio of the mantle as reported by Dreibus *et al.* (1995). Abbreviations as in Figs 1 and 2.

both S and Se were building in the magma owing to fractionation effects, additional $S^{2-}$ was being generated owing to the lowering of $fO_2$ and in turn the conversion of $SO_4^{2-}$ to $S^{2-}$ as a result of the increase in magnetite (see Fig. 3). However, S/Se ratios decrease from 875 m (at the top of LZc) to the base of the Cu zone because there was a decrease in the rate of S production owing to the fact that less cumulus magnetite was being formed (Fig. 11c). The sulphides at the base of UZa have low S/Se and Cu/Se ratios because the first cumulus sulphides to form at the base of the Cu zone would have been preferentially enriched in Se relative to S; it should be noted that there was a significant increase in the amount of cumulus sulphides being formed at the base of the Cu zone (see Fig. 6). However, both S/Se and Cu/Se increase through UZa and UZb because much of the Se had already been removed in the earlier-formed sulphides. Virtually all the Skaergaard rocks have S/Se ratios that are less than the normal mantle range (Fig. 11).

As it is possible to explain the variations in both S/Se and Cu/Se ratios in the Upper Zone in terms of the high partition coefficient of Se, there are no grounds on which to assume that there was post-cumulus loss or remobilization of S. Moreover, the strong correlation between Se and $P_2O_5$ does not support the suggestion of Andersen (2006) that S was leached from rocks below the Platinova Reef as a consequence of the conversion of pyrrhotite–chalcopyrite assemblages to bornite–chalcocite assemblages and added to the rocks above the Platinova Reef.

Although this study has indicated that there was no post-magmatic S loss from the Skaergaard, both the modelling of the behaviour of components in the fractionating melt and the analysis of its chilled margin indicate that the S content of the Skaergaard magma (~100 ppm) was significantly lower than that of most basaltic magmas. For example, sulphide-saturated MORB magmas contain 1000–1800 ppm S (Mathez, 1976) and the sulphide-undersaturated high-FeO magmas that produced the Deccan Traps flood basalts had up to 1400 ppm S (Self *et al.*, 2008; Keays & Lightfoot, 2010). One possible explanation for the low S content of the Skaergaard magma is that the mantle reservoir from which it was sourced had a low S content. Momme *et al.* (2006) concluded that the high-$TiO_2$ plateau basalts of East Greenland with which the Skaergaard is closely spatially linked were formed from magmas that had been sourced from a mantle reservoir that had a S content of 100 ppm, a value that is less than half that of the average 250 ppm S content of the mantle (Sun & McDonough, 1989). Our analysis of the Skaergaard data suggests that the Skaergaard magma was derived from a mantle reservoir that had an even lower S content.

## Pd/Pt ratios—products of extreme fractionation

A distinctive feature of the Au–PGE mineralization of the Platinova Reef is that it has high Pd/Pt ratios, with an average Pd/Pt ratio of ~10 (Andersen *et al.*, 1998). The mineralization has very low Ir, Ru and Rh (Supplementary Data Table 1).

The Pd/Pt ratio of the initial Skaergaard magma estimated from the Rayleigh fractionation modeling is 2·08 (Table 2); this value is considerably higher than that of the fertile primitive mantle, which has a Pd/Pt ratio of 0·80–0·92 (Becker *et al.*, 2006). As seen in Table 2, the Skaergaard magma also had a higher Pd/Pt ratio than the most primitive members of both the high-$TiO_2$ series (Pd/Pt = 1·11) and the low-$TiO_2$ series (Pd/Pt = 1·66) continental flood basalts of East Greenland studied by Momme *et al.* (2002). The high Pd/Pt ratio of the initial Skaergaard magma indicates that it had undergone a significant amount of differentiation before it entered the high-level magma chamber. As shown by Momme *et al.* (2002) and Lightfoot & Keays (2005), Pd/Pt ratios in S-undersaturated magmas increase during differentiation because the bulk partition coefficient (=metal in solids/metal in silicate liquid) of Pd is ~0·4, and that of Pt is ~1·0. Once inside the Skaergaard magma chamber, Pd/Pt ratios continued to increase as the magma crystallized (see Fig. 8b). By the time the Platinova Reef formed, the Pd/Pt ratio had increased to ~10.

There are, however, reversals in Pd/Pt ratio, the most notable being the rapid decrease from 988 m to 1024 m immediately below the Platinova Reef (Fig. 8b); this reversal is a regional feature that has been observed in other drill holes (Andersen *et al.*, 1998). In the stratigraphic reference section that we studied this interval also exhibits a rapid decrease in Pd, Pt and Au (Fig. 5). Of significance are the very rapid decreases in $FeO_T$, $TiO_2$ and V over the same interval (Fig. 3). As suggested by Holwell & Keays (2014), this indicates that the Fe–Ti oxides exerted a major control over the formation of the Cu–Au–PGE sulphides. The low magnetite content indicates that this was an interval of low $S^{2-}$ production from $(SO_4)^{2-}$ and that FeO continued to build up in the residual magma. In essence, the Pd/Pt ratios in this interval revert to what they were lower in the stratigraphy and before the formation of cumulus magnetite.

## Formation of the Platinova Reef

Bird *et al.* (1991) suggested that the Platinova Reef was formed via a filter pressing process in which Au and other incompatible elements built up in the intercumulus melt and migrated upwards through the overlying cumulates; they suggested that this process ultimately resulted in the exsolution of immiscible sulphide and precious metal liquids. Andersen *et al.* (1998), Nielsen *et al.* (2005) and Andersen (2006) suggested that all of the PGE and Au were captured by immiscible sulphide melts that were deposited in the TG-0 unit, the lowest felsic macro-layer of the Triple Group. Andersen *et al.* (1998) argued that the upwards decrease in Pd/Au ratios through the different layers of the Platinova Reef was due to upwards migration of both silicate interstitial melt and the PGE–Au-rich sulphide melt, which

fractionated as they moved upwards from TG-0. Andersen (2006) suggested that the systematic separation of Pd- and Au-rich layers in the Platinova Reef was due to mobilization of S, Pd and Au by late-stage magmatic or hydrothermal fluids that interacted with and dissolved the initial PGE- and Au-rich magmatic sulphides. Andersen (2006) further argued that the fluids migrated upwards through the overlying cumulates and deposited the metals at redox fronts within them; he also argued that the Pd–Au zoning is a product of the greater solubility of Au in hydrothermal fluids compared with Pd. Godel *et al.* (2014) proposed that the PGE-rich sulphides formed *in situ* as cumulus sulphide liquids during the formation and crystallization of Fe–Ti oxides; they rejected outright any possibility that the PGE-rich mineralization was a product of hydrothermal processes. In contrast, Godel *et al.* (2014) concluded that the Au zone may have precipitated from high-temperature, late magmatic, Cl-rich fluids, or was a product of differentiation of the magma. Holwell & Keays (2014), on the other hand, suggested that the entire Platinova Reef package was formed from a single Au–PGE-rich layer of magma at the base of the chamber and that the zoning of Au and Pd is due to the contrasting mineral/melt partition coefficients of Au and Pd.

Fractionation of a sulphide melt as it migrated upwards, as suggested by Andersen *et al.* (1998), should have produced an upward trend of increasing Cu/Se ratios because of the differences in the monosulphide solid solution (Mss)/sulphide melt partition coefficients between Cu ($D_{Cu}^{mss/sul\,melt} = 0{\cdot}2$; Ebel & Naldrett, 1996; Ballhaus *et al.*, 2001; Mungall *et al.*, 2005) and Se ($D_{Se}^{mss/sul\,melt} = 0{\cdot}65$; Helmy *et al.*, 2010). However, there is a decrease in Cu/Se ratios upwards through the Platinova Reef (Fig. 9c), which provides a strong argument against the variations in metal distribution being a product of fractionation of a sulphide melt. Because both Pd and Pt have low partition coefficients ($D_{Pd}^{mss/sul\,melt} = 0{\cdot}18$, $D_{Pt}^{mss/sul\,melt} = 0{\cdot}16$; Ballhaus *et al.*, 2001), a fractionating sulphide melt would produce sulphides that were increasingly Pd and Pt rich upwards, which is also not the case.

If S, Pd and Au had been redistributed by hydrothermal fluids as suggested by Andersen (2006), there also would have been significant redistribution of Se, which shows a very tight geochemical coherence with S at elevated temperatures (Yamamoto, 1976). However, there is only a very slight increase in Se/$P_2O_5$ ratios upwards through the Platinova Reef (Fig. 9d). As both $P_2O_5$ and the bulk of the Se in the rocks were contributed by the trapped interstitial melt, the good cohesion between Se and $P_2O_5$ rules out any significant remobilization of Se (and S) by hydrothermal fluids.

Holwell & Keays (2014) argued that the smooth upwards decrease in Pd/Au ratios through the Platinova Reef is consistent with segregation of magmatic sulphide melts from the base upwards from a PGE- and Au-rich layer of magma. However, comparison of Fig. 9a with Fig. 8c shows that the variations in Pd/Au ratios through the Platinova Reef are clearly in alignment with variations in Pd/Au ratios throughout the entire Skaergaard intrusion. With the exception of the reversal at 1024 m (also shown by $FeO_T$, $TiO_2$), Pd/Au ratios increase sharply upwards from the base of LZc to the base of the Platinova Reef, at which point they drop rapidly through the Platinova Reef up to the Au zone. These variations are consistent with the first cumulus sulphides to segregate from the Skaergaard magma being richer in Pd relative to Au because Pd has a much larger sulphide melt/silicate melt partition coefficient than Au ($D_{Pd}^{sul\,melt/sil\,melt} = 2{\cdot}15 \times 10^5$ whereas $D_{Au}^{sul\,melt/sil\,melt} = 5{\cdot}91 \times 10^3$ at $fO_2 = 9{\cdot}58$; Mungall & Brenan (2014).

We suggest that the Platinova Reef is the product of gradual changes in the physical and chemical properties of the Skaergaard magma and that it marks the transition from a state wherein only the boundary layer between the magma and the crystal mush was sulphide saturated from LZc times to one in which the entire magma chamber was sulphide saturated from the Cu Zone upwards. Although the magma within the boundary layer became sulphide saturated at the base of LZc some 300 m below the Platinova Reef, the very small amounts of sulphides being formed did not deplete the main magma in Pd, Pt, Au and Cu. Hence, S together with Pd, Pt, Au and Cu continued to build up in the residual melt. The formation of the Platinova Reef commenced when 75% of the initial Skaergaard magma had undergone fractional crystallization and as a result there had been a significant build-up of incompatible elements in the residual melt.

The following changes in the Skaergaard magma led to the formation of the Platinova Reef.

1. Fractionation of the magma led to an increase in the S, Cu, PGE, Au and Fe contents of the residual magma.
2. The build-up of Cu in the residual magma owing to fractionation decreased the S content of the magma required to bring it to saturation in Cu-rich Cu–Fe sulphides.
3. The appearance of Fe–Ti oxides as cumulus phases had two important consequences: (a) the crystallization of cumulus magnetite lowered the $Fe^{3+}/Fe^{2+}$ ratio of the magma and hence its $fO_2$, which prompted the conversion of $SO_4^{2-}$ to $S^{2-}$; this combined with the build-up of total S in the magma owing to fractionation resulted in an increase in the amount of $S^{2-}$ present in the residual melt; (b) crystallization of ilmenite as well as magnetite decreased the rate of build-up of FeO in the magma and hence decreased the amount of S in the magma required to bring it to sulphide saturation.
4. Cooling of the magma from ~1140°C at the base of LZa to ~1075°C at the base of the Platinova Reef (see Thy *et al.*, 2009*b*) would have significantly lowered the S content of the magma required to bring it to sulphide saturation; the cooling effects of this ~65°C drop in the temperature of the magma would have

been enhanced by convection currents, which carried magma that was further cooled against the roof and walls of the Skaergaard chamber to its floor.

5. Prior to and during formation of the Platinova Reef, sulphide saturation was localized to the immediate vicinity of the crystallization front within the boundary layer between the magma and the crystal mush–cumulate pile.
6. During the final stages of formation of the Platinova Reef, the magma in the entire chamber became sulphide saturated; this resulted in the formation of the Cu zone that lies immediately above the Platinova Reef.

## CONCLUSIONS

In summary, the Skaergaard magma was driven to local sulphide saturation in a boundary layer owing to a number of factors including a decrease in temperature, the build-up of S, FeO and Cu in the residual melt during magmatic differentiation, and crystallization of Fe–Ti oxides that inhibited the build-up of FeO in the residual melt and caused the conversion of some $SO_4^{2-}$ to $S^{2-}$. The Skaergaard magma became sulphide saturated much earlier than predicted from its major element composition owing mainly to the build-up of Cu in the residual magma. Although only tiny amounts of Cu-rich sulphides segregated from the magma, these were very rich in Pd and Pt owing to the very high sulphide melt/silicate melt partition coefficients of these elements.

The Platinova Reef is the product of gradual changes in the physical and chemical condition of the Skaergaard magma. Neither fractionation of sulphide melts nor redistribution of metals via hydrothermal fluids played any role in the formation of the Platinova Reef. In addition, this study has found no evidence of post-magmatic S loss from the Skaergaard rocks.

## ACKNOWLEDGEMENTS

The authors thank Troels Nielsen for providing some of the samples and many stimulating and challenging discussions. They also thank James Brenan and Ian Campbell for useful comments on an earlier version of this paper. Ed Ripley is thanked for the determination of S in five of the samples, and Troy Richardson of the Geoscience Laboratories for the determination of PGE and Au in the samples. Steve Barnes and Alan Boudreau are thanked for their constructive reviews of this paper.

## FUNDING

This work was supported by NSERC (Natural Sciences and Engineering Research Council of Canada) grant to RRK.

## SUPPLEMENTARY DATA

Supplementary data for this paper are available at *Journal of Petrology* online.

## REFERENCES

Andersen, J. C. Ø. (2006). Postmagmatic sulfur loss in the Skaergaard Intrusion: Implications for the formation of the Platinova Reef. *Lithos* **92**, 198–221.

Andersen, J. C. Ø., Rasmussen, H., Nielsen, T. F. D. & Ronsbo, J. C. (1998). The Triple Group and the Platinova gold and palladium reefs in the Skaergaard Intrusion: stratigraphic and petrographic relations. *Economic Geology* **93**, 488–509.

Ballhaus, C., Tredoux, M. & Späth, A. (2001). Phase relations in the Fe–Ni–Cu–PGE–S system at magmatic temperature and application to the massive sulphide ores of the Sudbury Igneous Complex. *Journal of Petrology* **42**, 1911–1926.

Barker, A. K., Baker, J. A. & Peate, D. W. (2006). Interaction of the rifting East Greenland margin with a zoned ancestral Iceland plume. *Geology* **34**, 481–484.

Becker, H., Horan, M. F., Walker, R. J., Gao, S., Lorand, J.-P. & Rudnick, R. L. (2006). Highly siderophile element composition of the Earth's primitive upper mantle: Constraints from new data on peridotite massifs and xenoliths. *Geochimica et Cosmochimica Acta* **70**, 4528–4550.

Bernstein, S. & Nielsen, T. F. D. (2004). Chemical stratigraphy in the Skaergaard intrusion. *GEUS Report 2004/123*, 31pp.

Bird, D. K., Brooks, C. K., Gannicott, R. A. & Turner, P. A. (1991). A gold bearing horizon in the Skaergaard Intrusion, East Greenland. *Economic Geology* **86**, 1083–1092.

Bollingberg, K. (1995). Iron–titanium oxides in the Skaergaard intrusion. Cand. Scient. thesis, Copenhagen University, 113 pp.

Borisov, A. & Danyushevsky, L. (2011). The effect of silica contents on Pd, Pt and Rh solubilities in silicate melts: an experimental study. *European Journal of Mineralogy* **23**, 355–367.

Brooks, C. K. & Nielsen, T. F. D. (1978). Early stages in the differentiation of the Skaergaard magmas as revealed by a closely related suite of dike rocks. *Lithos* **11**, 1–14.

Brooks, C. K., Larsen, L. M. & Nielsen, T. F. D. (1991). Importance of iron rich tholeiitic magmas at divergent plate margins: a reappraisal. *Geology* **19**, 269–272.

Buddington, A. F. & Lindsley, D. H. (1964). Iron–titanium oxide minerals and their synthetic equivalents. *Journal of Petrology* **5**, 310–357.

Dreibus, G., Palme, H., Spettel, B., Zipfel, J. & Wanke, H. (1995). Sulfur and selenium in chondritic meteorites. *Meteoritics* **30**, 439–445.

Ebel, D. S. & Naldrett, A. J. (1996). Fractional crystallization of sulfide ore liquids at high temperature. *Economic Geology* **91**, 607–621.

Ewers, G. R. (1977). Experimental hot water-rock interactions and their significance to hydrothermal systems in New Zealand. *Geochimica et Cosmochimica Acta* **41**: 143-150.

Frost, B. R. & Lindsley, D. H. (1992). Equilibria among Fe–Ti oxides, pyroxenes, olivine, and quartz: Part II. Application. *American Mineralogist* **77**, 1004–1020.

Godel, B., Rudashevsky, N. S., Nielsen, T. F. D., Barnes, S. J. & Rudashevsky, V. N. (2014). New constraints on the origin of the Skaergaard Intrusion Cu–Pd–Au mineralization: Insights from high-resolution X-ray computed tomography. *Lithos* **190–191**, 27–36.

Haughton, D. R., Roeder, P. L. & Skinner, B. J. (1974). Solubility of sulfur in mafic magmas. *Economic Geology* **69**, 451–467.

Helmy, H. M., Ballhaus, C., Wohlgemuth-Ueberwasser, C., Fonseca, R.O.C., Laurenz, V. (2010). Partitioning of Se, As, Sb, Te and Bi between monosulfide solid solution and sulfide melt – Application to magmatic sulfide deposits. *Geochimica et Cosmochimica Acta* **74**, 6174–6179.

Hirschmann, M. M., Renne, P. R. & McBirney, A. R. (1997). $^{40}Ar$–$^{39}Ar$ dating of the Skaergaard intrusion. *Earth and Planetary Science Letters* **146**, 645–658.

Holwell, D. A. & Keays, R. R. (2014). The formation of low volume, high tenor magmatic PGE–Au sulfide mineralization in closed systems: evidence from precious and base metal geochemistry of the Platinova Reef, Skaergaard Intrusion, East Greenland. *Economic Geology* **109**, 387–406.

Holwell, D. A., Keays, R. R., Williams, M. R. & McDonald, I. (2015). Super-concentration of PGE, Au and Se by multi-stage concentration and dissolution of sulfide liquids: evidence from mineralogical and LA-ICP-MS analysis of sulfide droplets in the Skaergaard Intrusion, east Greenland. *Contributions to Mineralogy and Petrology* doi:10.1007/s00410-015-1203-y.

Hoover, J. D. (1989). Petrology of the Marginal Border Series of the Skaergaard intrusion. *Journal of Petrology* **30**, 399–439.

Hunter, R. H. & Sparks, R. S. J., (1987). The differentiation of the Skaergaard Intrusion. *Contributions to Mineralogy and Petrology* **95**, 451-461.

Irvine, T. N., Andersen, J. C. Ø. & Brooks, C. K. (1998). Included blocks (and blocks within blocks) in the Skaergaard intrusion: Geologic relations and the origins of rhythmic modally graded layers. *Geological Society of America Bulletin* **110**, 1398–1447.

Jackson, S. E., Fryer, B. J., Gosse, W., Healey, D. C., Longerich, H. P. & Strong, D. F. (1990). Determination of the precious metals in geological materials by inductively coupled plasma-mass spectrometry (ICP-MS) with nickel sulphide fire-assay collection and tellurium co-precipitation. *Chemical Geology* **83**, 119–132.

Jakobsen, J. K., Tegner, C., Brooks, C. K., Kent, A. J. R., Lesher, C. E., Nielsen, T. F. D. & Wiedenbeck, M. (2010). Parental magma of the Skaergaard intrusion: constraints from melt inclusions in primitive troctolite blocks and FG-1 dykes. *Contributions to Mineralogy and Petrology* **159**, 61–79.

Jenner, F. E., O'Neill, H. St. C., Arculus, R. J. & Mavrogenes, J. A. (2010). The magnetite crisis in the evolution of arc-related magmas and the initial concentration of Au, Ag and Cu. *Journal of Petrology* **51**, 2445–2464.

Jugo, P. J., Luth, R. W. & Richards, J. P. (2005). Experimental data on the speciation of sulfur as a function of oxygen fugacity in basaltic melts. *Geochimica et Cosmochimica Acta* **69**, 497–503.

Jugo, P. J., Wilke, M. & Botcharnikov, R. E. (2010). Sulfur K-edge XANES analysis of natural basaltic glasses: Implications for S speciation as function of oxygen fugacity. *Geochimica et Cosmochimica Acta* **74**, 5926–5938.

Keays, R. R. & Lightfoot, P. C. (2004). Formation of Ni–Cu–platinum group element sulphide mineralisation in the Sudbury impact melt sheet. *Mineralogy and Petrology* **82**, 217–258.

Keays, R. R. & Lightfoot, P. C. (2010). Crustal sulphur is required to form magmatic Ni–Cu sulphides: evidence from chalcophile element signatures of Siberian and Deccan Trap basalts. *Mineralium Deposita* **45**, 241–257.

Keays, R. R., Tegner, C., Momme, P. & Nielsen, T. F. D. (2008). Controls on the formation of Pd–Au mineralization in the Skaergaard intrusion, East Greenland. In: Proceedings of the 33rd International Geological Congress, Oslo, Norway, August 5–14, 2008.

Larsen, R. B. & Tegner, C. (2006). Pressure conditions for the solidification of the Skaergaard intrusion: Eruption of East Greenland flood basalts in less than 300,000 years. *Lithos* **92**, 181–197.

Li, C. & Ripley, E. M. (2009). Sulfur contents at sulfide–liquid or anhydrite saturation in silicate melts: empirical equations and example applications. *Economic Geology* **104**, 405–412.

Lightfoot, P. C. & Keays, R. R. (2005). Siderophile and chalcophile metal variations in flood basalts from the Siberian Trap, Noril'sk Region: Implications for the origin of the Ni–Cu–PGE sulfide ores. *Economic Geology* **100**, 439–462.

Mathez, E.A. (1976). Sulfur solubility and magmatic sulfides in submarine basalt glass. *Journal of Geophysical Research* **81**, 4269-4276.

McBirney, A. R. (1995). Mechanisms of differentiation in the Skaergaard Intrusion. *Journal of the Geological Society, London* **152**, 421–435.

McBirney, A. R. (1996). The Skaergaard intrusion. In: Cawthorn, R. G. (ed.) *Layered Intrusions. Developments in Petrology, Vol. 15*. Elsevier, pp. 147–180.

McBirney, A. R. & Creaser, R.A. (2003). The Skaergaard Layered Series, Part VII: Sr and Nd Isotopes. *Journal of Petrology* **44**, 757-771.

McDonald, A. M., Cabri, L. J., Rudashevsky, N. S., Stanley, C. J., Rudashevsky, V. N. & Ross, K. C. (2008). Nielsenite, $PdCu_3$, a new Platinum-group intermetallic mineral species from the Skaergaard Intrusion, Greenland. *Canadian Mineralogist* **46**, 709–716.

Momme, P. (2000). Flood basalt generation and differentiation. PGE-geochemistry of East Greenland flood basalts, comagmatic intrusions and comparison with Siberian flood basalts. Unpublished PhD Thesis, Aarhus University, Aarhus, Denmark.

Momme, P., Brooks, C. K., Tegner, C. & Keays, R. R. (2002). Platinum-group element behaviour in basalts from East Greenland rifted margin. *Contributions to Mineralogy and Petrology* **143**, 133–153.

Momme, P., Tegner, C., Brooks, C. K. & Keays, R. R. (2006). Two melting regimes during Paleogene flood basalt generation in East Greenland: combined REE and PGE modeling. *Contributions to Mineralogy and Petrology* **151**, 88–100.

Morse, S. A., Lindsley, D. H. & Williams, R. J. (1980). Concerning intensive parameters in the Skaergaard Intrusion. *American Journal of Science* **280A**, 159–170.

Mungall, J. E. & Brenan, J. M. (2014). Partitioning of platinum-group elements and Au between sulfide liquid and basalt and the origins of mantle–crust fractionation of the chalcophile elements. *Geochimica et Cosmochimica Acta* **125**, 265–289.

Mungall, J. E., Andrews, D. R. A., Cabri, L. J., Sylvester, P. J. & Tubrett, M. (2005). Partitioning of Cu, Ni, Au, and platinum-group elements between monosulfide solid solution and sulfide melt under controlled oxygen and sulfur fugacities. *Geochimica et Cosmochimica Acta* **69**, 4349–4360.

Naslund, H. R. (1984). Petrology of the Upper Border Series of the Skaergaard intrusion. *Journal of Petrology* **25**, 185–212.

Nielsen, T. F. D. (2004). The shape and volume of the Skaergaard intrusion, Greenland: implications for mass balance and bulk composition. *Journal of Petrology* **45**, 507–530.

Nielsen, T. F. D., Andersen, J. C. Ø. & Brooks, C. K. (2005). The Platinova Reef of the Skaergaard intrusion. In: Mungal, J. E. (ed.) *Exploration for Platinum Group Element Deposits. Mineralogical Association of Canada Short Course Series* **35**, 431–455.

Nielsen, T. F. D. & Brooks, C.K. (1995). Precious metals in magmas fo East Greenland:Factors important to the mineralization in the Skaergaard Intrusion. *Economic Geology* **90**, 1911-1917.

Norton, D. & Taylor, H. P. (1979). Quantitative simulation of the hydrothermal systems of crystallizing magmas on the basis of transport theory and oxygen isotope data: An analysis of the Skaergaard intrusion. *Journal of Petrology* **20**, 421–486.

O'Neill, H. S. C. & Mavrogenes, J. A. (2002). The sulfide capacity and the sulfur content at sulfide saturation of silicate melts at 1400°C and 1 bar. *Journal of Petrology* **43**, 1049–1087.

Peach, C. L., Mathez, E. A. & Keays, R. R. (1990). Sulphide melt–silicate melt distribution coefficients for the noble metals and other chalcophile metals as deduced from MORB:

Implications for partial melting. *Geochimica et Cosmochimica Acta* **54**, 3379–3389.

Peate, D. W. & Stecher, O. (2003). Pb isotope evidence for contributions from different Iceland mantle components to Palaeogene East Greenland flood basalts. *Lithos* **67**(**1–2**), 39–52.

Peate, D. W., Baker, J. A., Blichert-Toft, J., Hilton, D. R., Storey, M., Kent, A. J. R., Brooks, C. K., Hansen, H., Pedersen, A. K. & Duncan, R. A. (2003). The Prinsen af Wales Bjerge Formation lavas, East Greenland: the transition from tholeiitic to alkalic magmatism during Palaeogene continental break-up. *Journal of Petrology* **44**(**2**), 279–304.

Pedersen, A. K., Watt, M., Watt, W. S. & Larsen, L. M. (1997). Structure and stratigraphy of the Early Tertiary basalts of the Blosseville Kyst, East Greenland. *Journal of the Geological Society, London* **154**, 565–570.

Ripley, E., Brophy, J. G. & Li, C. S. (2002). Copper solubility in a basaltic melt and sulfide liquid/silicate melt partition coefficients of Cu and Fe. *Geochimica et Cosmochimica Acta* **66**, 2791–2800.

Ripley, E., Li, C., Moore, C. H., Elswick, E. R., Maynard, J. B., Paul, R. L., Sylvester, P., Seo, J. H. & Shimizu, N. (2011). Analytical methods for sulfur determination in glasses, rocks, minerals and fluid inclusions. In: Behrens, H. & Webster, J. D. (eds) *Sulfur in Magmas and Melts: Its Importance for Natural and Technical Processes. Mineralogical Society of America and Geochemical Society, Reviews in Mineralogy and Geochemistry* **73**, 9–39.

Rollinson, H. R. (1993). *Using geochemical data: evaluation, presentation, interpretation*. Harlow, England, Longman.

Rudashevsky, N. S., McDonald, A. M., Cabri, L. J., Nielsen, T. F. D., Stanley, C. J., Kretser, Y. L. & Rudashevsky, V. N. (2004). Skaergaardite, PdCu, a new platinum-group intermetallic mineral from the Skaergaard Intrusion, Greenland. *Mineralogical Magazine* **68**, 615–632.

Rudashevsky, N. S., Rudashevsky, V. N. & Nielsen, T. F. D. (2010). *Gold, PGE and sulphide phases of the precious metal mineralization of the Skaergaard intrusion: Part 9, sample 90-18, 978. Geological Survey of Denmark and Greenland Report* **2010/74**, 21 pp.

Salmonsen, L. P. & Tegner, C. (2013). Crystallization sequence of the Upper Border Series of the Skaergaard Intrusion: revised subdivision and implications for chamber-scale magma homogeneity. *Contributions to Mineralogy and Petrology* **165**, 1155–1171.

Sato, M. & Valenza, M. (1980). Oxygen fugacities of the Layered Series of the Skaergaard intrusion, East Greenland. *American Journal of Science* **280-A**, 134–158.

Self, S., Blake, S., Sharma, K., Widdowson, M. & Sephton, S. (2008). Sulfur and chlorine in Late Cretaceous Deccan magmas and eruptive gas release. *Science* **319**, 1654–1657.

Storey, M., Pedersen, A. K., Stecher, O., Bernstein, S., Larsen, H. C., Larsen, L. M., Baker, J. A. & Duncan, R. A. (2004). Long-lived postbreakup magmatism along the East Greenland margin: Evidence for shallow-mantle metasomatism by the Iceland plume. *Geology* **32**, 173–176.

Storey, M., Duncan, R. A. & Tegner, C. (2007). Timing and duration of volcanism in the North Atlantic Igneous Province: Implications for geodynamics and links to the Iceland hotspot. *Chemical Geology* **241**, 264–281.

Sun, S.-S. & McDonough, W. F. (1989). Chemical and isotopic systematics of oceanic basalts: implications for mantle composition and processes. In: Saunders, A. D. & Norry, M. J. (eds) *Magmatism in the Ocean Basins. Geological Society, London, Special Publications* **42**, 313–345.

Taylor, H. P. & Forester, R. W. (1979). An oxygen and hydrogen isotope study of the Skaergaard intrusion and its country rocks: A description of a 55 my old fossil hydrothermal system. *Journal of Petrology* **20**, 355–419.

Tegner, C. (1997). Iron in plagioclase as a monitor of the differentiation of the Skaergaard Intrusion. *Contributions to Mineralogy and Petrology* **128**, 45–51.

Tegner, C. & Cawthorn, R. G. (2010). Iron in plagioclase in the Bushveld and Skaergaard intrusions: implications for iron contents in evolving basic magmas. *Contributions to Mineralogy and Petrology* **159**, 719–730.

Tegner, C., Lesher, C. E., Larsen, L. M. & Watt, W. S. (1998). Evidence from the rare-earth-element record of mantle melting for cooling of the Tertiary Iceland plume. *Nature* **395**(**6702**), 591–594.

Tegner, C., Thy, P., Holness, M. B., Jakobsen, J. K. & Lesher, C. E. (2009). Differentiation and compaction in the Skaergaard Intrusion. *Journal of Petrology* **50**, 813–840.

Thy, P., Lesher, C. E. & Tegner, C. (2009*a*). The Skaergaard liquid line of descent revisited. *Contributions to Mineralogy and Petrology* **157**(**6**), 735–747.

Thy, P., Tegner, C. & Lesher, C. E. (2009*b*). Liquidus temperatures of the Skaergaard magma. *American Mineralogist* **94**, 1371–1376.

Toplis, M. J. & Carroll, M. R. (1996). Differentiation of ferro-basaltic magmas under conditions open and closed to oxygen: implications for the Skaergaard intrusion and other natural systems. *Journal of Petrology* **37**, 837–858.

Turner, P. A. (1986). The sulfide mineralogy and the behavior of S and certain trace elements in the Skaergaard Intrusion, East Greenland. Masters thesis, Dartmouth College, Hanover, New Hampshire, 79 pp.

Vincent, E.A. & Crocket, J.H., 1960, Studies in the geochemistry of gold-1 The distribution of gold in rocks and minerals of the Skaergaard intrusion, East Greenland. *Geochimica et Cosmochimica Acta* **18**, 130-142.

Vincent, E.A. & Smales, A.A. (1956) The determination of palladium and gold in igneous rocks by radioactivation analysis. *Geochimica et Cosmochimica Acta* **9**, 151-160.

Wager, L. R. & Brown, G. M. (1968). *Layered Igneous Rocks*. Oliver & Boyd.

Wager, L. R. & Deer, W.A. (1939) Geological investigations in East Greenland, Part III. The petrology of the Skaergaard Intrusion, Kangerdlugssuaq, East Greenland, *Meddelelser om Grønland* **105**, 1-352

Wager, L. R., Vincent, E. A. & Smales, A. A. (1957). Sulphides in the Skaergaard Intrusion, East Greenland. *Economic Geology* **52**, 855–903.

White, R. & McKenzie, D. (1995) Mantle plumes and flood basalts. *Journal of Geophysical Research* **100**, 17543–17585.

Wilson, J. T. (1973). Mantle plumes and plate motions. *Tectonophysics* **19**, 149–164.

Wohlgemuth-Ueberwasse, C. C., Fonseca, R. O., Ballhaus, C. & Berndt, J. (2013). Sulfide oxidation as a process for the formation of copper-rich magmatic sulfides. *Mineralium Deposita* **48**, 115–127.

Wotzlaw, J.-F., Bindeman, I. N., Schaltegger, U., Brooks, C. K. & Naslund, H. R. (2012). High-resolution insights into episodes of crystallization, hydrothermal alteration and remelting in the Skaergaard intrusive complex. *Earth and Planetary Science Letters* **355–356**, 199–212.

Yamamoto, M. (1976). Relationship between Se/S and sulfur isotope ratios of hydrothermal sulfide minerals. *Mineralium Deposita* **11**, 197–209.